https://doi.org/10.5194/egusphere-2026-5442
Preprint. Discussion started: 10 September 2026

The air-sea CO_2 fluxes and ship CO_2 emissions in the Baltic Sea during 2019–2021, using in-situ and inversion methods

Vertti Kettunen[1], Tuula Aalto[2], Henry C. Bittig[4], Jukka-Pekka Jalkanen[3], Lauri Laakso[1,5], Anteneh Mengistu[2], Gregor Rehder[4], Maria Tenkanen[2], and Martti Honkanen[1]

[1]Meteorological and Marine Research Programme, Finnish Meteorological Institute, Helsinki, Finland
[2]Climate System Research Programme, Finnish Meteorological Institute, Helsinki, Finland
[3]Atmospheric Composition Research Programme, Finnish Meteorological Institute, Helsinki, Finland
[4]Leibniz Institute for Baltic Sea Research Warnemünde (IOW), Rostock-Warnemünde, Germany
[5]School of Physical and Chemical Sciences, North-West University, Potchefstroom Campus, South Africa

Correspondence: Vertti Kettunen (vertti.kettunen@fmi.fi)

Abstract. Estimating air–sea CO_2 exchange in coastal and semi-enclosed seas is challenging due to limited spatial and temporal observational coverage. Atmospheric inverse modelling offers a complementary approach, although its ability to resolve regional marine carbon fluxes is still uncertain. In the Baltic Sea, intensive shipping further complicates the regional carbon budget through substantial anthropogenic CO_2 emissions. This study presents one of the first assessments combining air–sea CO_2 exchange and ship-derived CO_2 emissions in the Baltic Sea using both observation-based and atmospheric inversion approaches.

Air–sea CO_2 fluxes for 2019 to 2021 were estimated using two independent methods. The first method combined a bulk flux calculation, which includes sea–air pCO_2 differences, wind-speed-dependent gas transfer velocity, solubility, and sea-ice cover, with shipping emissions simulated by the Ship Traffic Emission Assessment Model (STEAM). The second method used atmospheric CO_2 observations together with atmospheric transport modelling in the CIF-FLEXPART inversion framework to estimate surface CO_2 fluxes, providing an alternative observation-based approach. The results were analyzed for the entire Baltic Sea and for 13 HELCOM sub-basins.

The STEAM-corrected bulk method indicated that the Baltic Sea acted as a net CO_2 sink during 2019 to 2021, with a mean flux of -1.79 $\mathrm{mmol\,m^{-2}\,d^{-1}}$. Without shipping emissions, the estimated flux was -3.76 $\mathrm{mmol\,m^{-2}\,d^{-1}}$, showing that ship traffic increased the net flux by approximately 1.97 $\mathrm{mmol\,m^{-2}\,d^{-1}}$. In contrast, the CIF-FLEXPART inversion estimated a net source of 3.92 $\mathrm{mmol\,m^{-2}\,d^{-1}}$ for the Baltic Sea. The climatological bulk-flux estimate for 2003 to 2021, excluding shipping emissions, gave a near-neutral mean flux of 0.25 $\mathrm{mmol\,m^{-2}\,d^{-1}}$. The basin-scale monthly fluxes showed moderate overall agreement between the two methods (mean Pearson correlation $r = 0.49$), with stronger correlations ($r = 0.62$–0.79) in several southern basins where observational coverage was greatest.

The contrasting estimates of the Baltic Sea carbon balance show that considerable uncertainties remain in both bulk method and inversion method approaches and that shipping emissions need to be taken into account. More continuous and reliable observations, improved representation of coastal carbon processes, and further development of atmospheric inversion systems are needed to better constrain regional marine carbon budgets.

https://doi.org/10.5194/egusphere-2026-5442
Preprint. Discussion started: 10 September 2026

1 Introduction

Oceanic carbon storage is approximately 60 times larger than atmospheric carbon storage (Sarmiento and Gruber, 2006), underscoring the critical function of the oceans in the global carbon cycle. Therefore, a comprehensive understanding of air–sea carbon dynamics is necessary to accurately quantify the global carbon budget and to assess strategies for achieving the objectives of the Paris Climate Agreement. Since the onset of industrialization, carbon dioxide (CO_2) has emerged as the predominant anthropogenic greenhouse gas.

The air–sea CO_2 flux is primarily determined by the difference in the partial pressure of carbon dioxide between the atmosphere and the sea surface (ΔpCO_2), while gas transfer velocity and solubility also influence the flux. Partial pressure is linked to concentration through solubility, which depends on salinity and temperature. Because atmospheric pCO_2 exhibits relatively minor variability (Rutgersson et al., 2009) compared to seawater pCO_2 in coastal regions, the partial pressure of carbon dioxide in seawater (pCO_2^{sea}) is the principal factor controlling ΔpCO_2 variability. The direction of the air–sea CO_2 flux depends on the sign of the partial pressure difference: when pCO_2^{sea} exceeds pCO_2^{atm}, the sea acts as a source of CO_2 to the atmosphere; conversely, when pCO_2^{sea} is lower than pCO_2^{atm}, the ocean acts as a sink.

The pCO_2^{sea} demonstrates pronounced seasonal (Müller and Schneider, 2018; Rutgersson et al., 2008; Schneider et al., 2006) and interannual variability (Schneider et al., 2014; Honkanen et al., 2024), typically ranging from approximately 100 to 500 µatm under pelagic conditions in the Eastern Gotland Basin. As a result, air–sea CO_2 fluxes are generally negative (sink) during spring and summer, and positive (source) during autumn and winter. Increased solar radiation in spring intensifies photosynthesis in the surface layer, which reduces seawater CO_2 concentration and enhances atmospheric CO_2 uptake. The first annual minimum in CO_2 concentration usually occurs in May, depending on location (Müller and Schneider, 2018). A second minimum often occurs in early July, when nitrogen fixation stimulates phytoplankton growth and further depletes inorganic carbon. In autumn, declining solar radiation weakens thermal stratification and promotes vertical mixing, transporting carbon-rich waters from deeper layers to the surface. These well-mixed conditions typically persist from late autumn until the onset of the subsequent spring bloom (Leppäranta and Myrberg, 2009).

The Baltic Sea, situated in Northern Europe, is relatively small on a global scale, yet it serves as a significant case study for the carbon cycle in brackish seas worldwide. Its extensive catchment area (1.7 million km^2), numerous freshwater river inflows, connection to the Atlantic Ocean, and complex ecosystem distinguish it as a unique region for such investigations. Additionally, the Baltic Sea region is marked by dense human populations, widespread agriculture and forestry, valuable marine resources, and intensive shipping activity, all of which are integral to regional economies. These features make the Baltic Sea an important system for examining regional carbon cycling and assessing the impact of ship emissions.

Air–sea CO_2 fluxes, both net and local, in the Baltic Sea have been investigated using various methods. Studies by Kuliński and Pempkowiak (2011); Gustafsson et al. (2014); Norman et al. (2013) used reanalyses and numerical simulations, while Parard et al. (2017) used remote sensing techniques. In addition, Lansø et al. (2015) compiled and compared results from

https://doi.org/10.5194/egusphere-2026-5442
Preprint. Discussion started: 10 September 2026

several studies, including their own analyses. Reported net air–sea flux estimates range from -1.2 to 0.6 $\mathrm{mmol\,m^{-2}\,d^{-1}}$. Gutiérrez-Loza et al. (2021) provided several estimates of net flux values for 2009–2011, with results between -0.53 and 0.0 $\mathrm{mmol\,m^{-2}\,d^{-1}}$. Furthermore, Jalkanen et al. (2009) estimated CO_2 emissions from Baltic Sea shipping at 19 Mt in 2007 using the STEAM model. When distributed over the Baltic Sea area (422,000 km^2), this correlates to an average flux of approximately 2.8 $\mathrm{mmol\,m^{-2}\,d^{-1}}$. The biogenic estimates of net air–sea CO_2 fluxes span negative to positive values, indicating that the Baltic Sea's role as a net sink or source of CO_2 remains uncertain and is likely subject to interannual variability.

In bulk flux calculations, the STEAM model (Jalkanen et al., 2009) was employed to estimate the influence of ship emissions on the marine carbon balance. This approach uses automatic identification system position reports, incorporates vessel technical specifications, and accounts for environmental conditions. The explicit inclusion of ship emissions in Baltic Sea CO_2 flux studies has not been previously addressed.

Previous studies have provided valuable information on the carbon cycle of the Baltic Sea. However, most previous estimates have been based on oceanographic observations, numerical simulations, or remote sensing products. Atmospheric inverse models have also been applied to estimate oceanic CO_2 fluxes, but their spatial resolution has generally been insufficient for regional studies of the Baltic Sea (Chandra et al., 2022; Friedlingstein et al., 2026). Atmospheric inverse models infer surface CO_2 fluxes from atmospheric concentration measurements and atmospheric transport modelling. First, an initial estimate of spatially distributed greenhouse gas fluxes (prior fluxes) is provided to a three-dimensional atmospheric transport model that simulates how greenhouse gases are transported through the atmosphere. The resulting modelled concentrations are then compared to measurements. When a mismatch between the modelled and measured atmospheric greenhouse gas concentrations is found, the inverse model adjusts the prior fluxes using Bayesian statistics. The optimised fluxes (posterior fluxes) include information of all the sources and sinks in the region.

This study investigates air–sea CO_2 flux and ship emissions in the Baltic Sea during 2019–2021 using two independent approaches: wind speed-based parameterization (bulk) combined with the ship traffic emission assessment model (hereafter referred to as the STEAM-corrected bulk method) and the CIF-FLEXPART inverse model. Additionally, we perform CO_2 flux calculations based on climatological data from 2003 to 2021 using the bulk method. The study further aims to compare the flux estimates obtained from these methods and assess their spatial and temporal consistency.

2 Materials and Methods

2.1 Calculation of air–sea CO_2 flux

In addition to the partial pressure gradient between the air and sea, the gas transfer velocity k [cm h^{-1}] and the solubility K_0 [mol L^{-1} atm^{-1}] are critical factors influencing the air–sea CO_2 flux. The regional fraction of sea ice cover, f, is incorporated to represent the reduction in air–sea CO_2 exchange during winter. Consistent with prevailing assumptions in the literature, air–sea CO_2 exchange over ice-covered areas is considered negligible. The bulk flux equation utilized in this study is:

https://doi.org/10.5194/egusphere-2026-5442
Preprint. Discussion started: 10 September 2026

$$F = kK_0\Delta pCO_2(1-f) \quad (1)$$

Numerous parameterizations have been proposed for the gas transfer velocity, k, most of them based on wind speed (Wanninkhof, 1992; Wanninkhof and McGillis, 1999; Weiss et al., 2007). In the Baltic Sea, wind speed remains the dominant predictor of k, although recent research indicates that the relationship between k and wind speed is modulated by local sea-state conditions. Specifically, limited fetch and increased surfactant concentrations can decrease k compared to open-ocean parameterizations, particularly in coastal regions (Dong et al., 2026; Dobashi et al., 2026). The influence of various physical processes on gas transfer velocity has also been examined by Gutiérrez-Loza et al. (2021) and Bock et al. (1999). This study employs the widely used parameterization introduced by Wanninkhof (1992) and updated by Wanninkhof (2014), as it has been extensively applied in Baltic Sea research and provides a robust basis for comparison with previous estimates:

$$k = k_{660}(u)\left(\frac{660}{Sc(T,s)}\right)^{1/2} \quad (2)$$

where

$$k_{660} = 0.251u_{10}^2 \quad (3)$$

The Schmidt number (Sc) quantifies the capacity of a gas molecule to cross the laminar boundary layer, with its value dependent on temperature (T) and salinity (s). The variable u_{10} represents wind speed measured at a height of 10 meters. The parameterization of the Schmidt number is detailed in Wanninkhof (2014).

The solubility coefficient K_0, which depends on temperature and salinity, was first introduced by Weiss (1970) and subsequently revised by Weiss (1974). The parameterization of K_0 incorporates several empirical coefficients specifically defined for CO_2.

The atmospheric partial pressure of CO_2 (pCO_2^{atm}) is parameterized using the approach of Rutgersson et al. (2009), which is based on the atmospheric carbon dioxide mole fraction and adjusted to reflect conditions at 100% relative humidity, as described by Dickson et al. (2007). This parameterization incorporates the long-term global trend, anthropogenic influences, and the natural seasonal cycle of carbon dioxide, and is directly applicable to the Baltic Sea. The anthropogenic component represents the estimated contribution of human activities to atmospheric CO_2, calculated as the deviation from the global atmospheric trend as a function of latitude. As a result, local increases in atmospheric CO_2 concentrations, such as those arising from major shipping routes or harbors, are not explicitly included. These local enhancements in atmospheric pCO_2 would alter the air-sea partial pressure gradient and, therefore, the estimated air-sea CO_2 flux. The calculation of pCO_2^{atm} requires, in addition to latitude, variables such as time (in years), day of year, and surface air pressure over the sea.

https://doi.org/10.5194/egusphere-2026-5442
Preprint. Discussion started: 10 September 2026

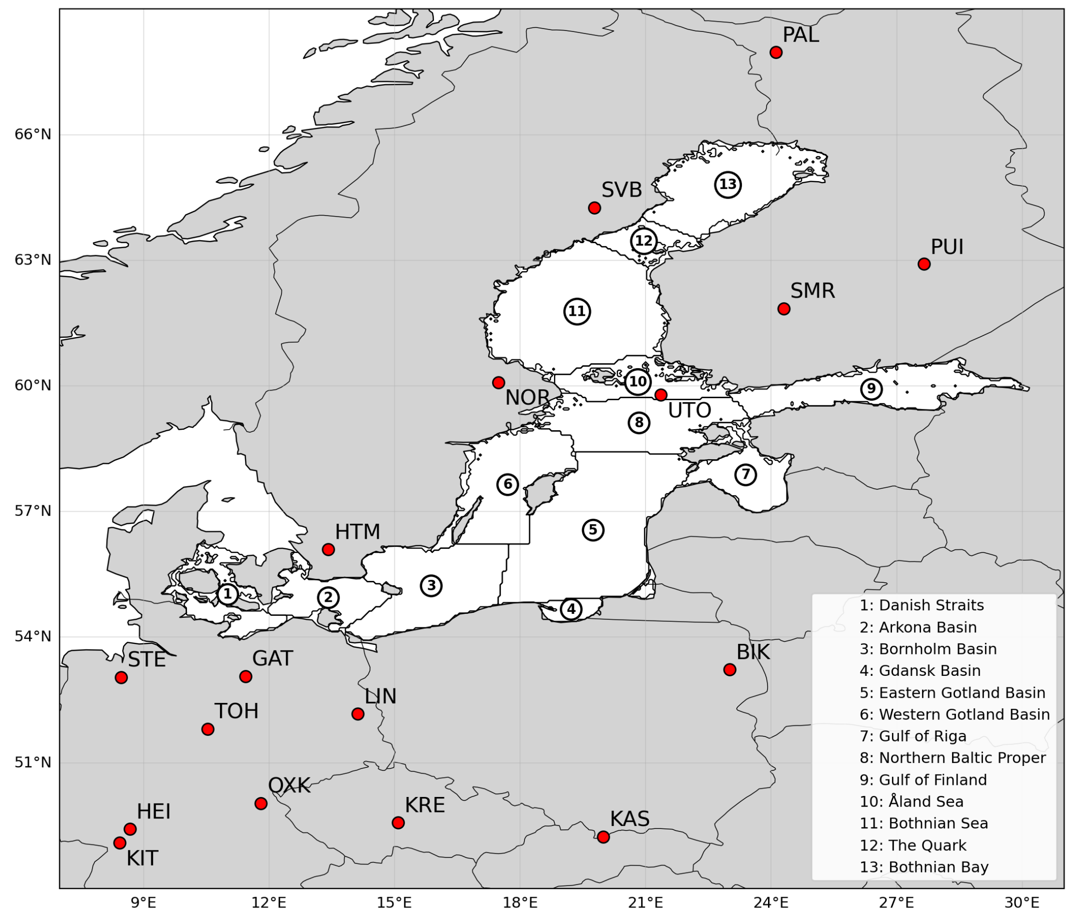

Figure 1. Map of the Baltic Sea and the sub-basins used in the calculations. Red dots indicate the CO_2 observation sites used in the inverse model. Seventeen observation sites are visible within the map extent. The observation sites shown are BIK (Białystok, Poland), GAT (Gartow, Germany), HEI (Heidelberg, Germany), HTM (Hyltemossa, Sweden), KAS (Kasprowy Wierch, Poland), KIT (Karlsruhe, Germany), KRE (Košetice, Czech Republic), LIN (Lindenberg, Germany), NOR (Norunda, Sweden), OXK (Ochsenkopf, Germany), PAL (Pallas, Finland), PUI (Puijo, Kuopio, Finland), SMR (Hyytiälä, Juupajoki, Finland), STE (Steinkimmen, Germany), SVB (Svartberget, Sweden), TOH (Torfhaus/Harz, Germany), and UTO (Utö, Finland).

2.2 Datasets used to calculate the air–sea CO_2 flux

STEAM-corrected bulk method air–sea CO_2 flux estimates were obtained from multiple observational and reanalysis datasets. Figure 2 provides a schematic overview of the calculation procedure and the data sources utilized at each stage. The final spatial resolution is 0.1° within the domain 52° to 66°N and 9° to 31°E. The temporal resolution of the data is one month. Due to differing spatial resolutions among the source data matrices, spatial averaging was performed to harmonize the datasets into a consistent format. All datasets were aggregated to a common 0.1° grid using bin averaging.

https://doi.org/10.5194/egusphere-2026-5442
Preprint. Discussion started: 10 September 2026

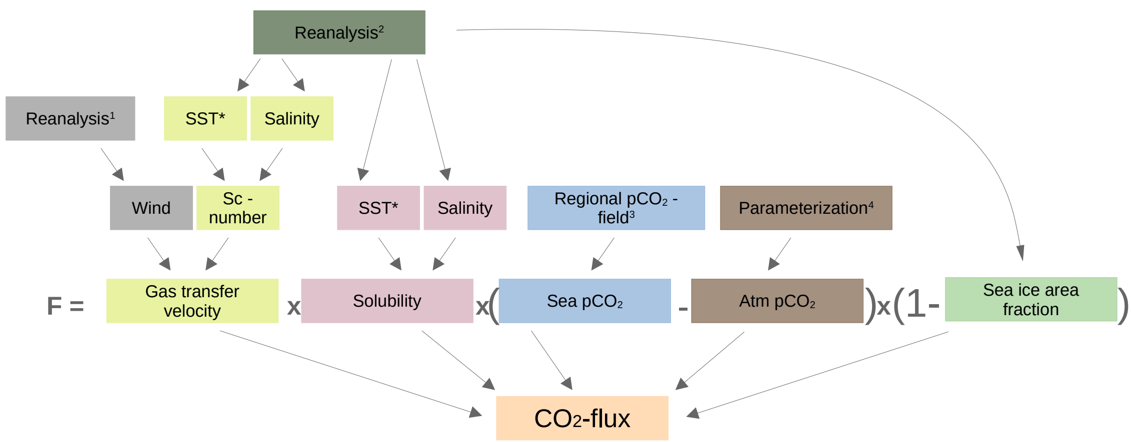

Figure 2. Schematic overview of the data sources and the calculation process for the CO_2 bulk flux. SST indicates sea surface temperature, and Sc-number represents the Schmidt number. The sources for each variable are listed in the bottom right corner. Following the calculation of the bulk air-sea CO_2 flux, the STEAM flux is incorporated.

Two reanalysis datasets were utilized for the CO_2 flux calculations: the E.U. Copernicus Marine Service Information; Baltic Sea Physics Reanalysis (Danish Meteorological Institute (DMI), 2023) for salinity and sea surface temperature, and the Copernicus European Regional Reanalysis (CERRA) (Schimanke et al., 2021) for wind data. The Baltic Sea Physics Reanalysis is derived from the NEMO (Nucleus for European Modelling of the Ocean) ice-ocean model system and integrates satellite observations with in situ measurements. The CERRA reanalysis is refined from the global ERA5 reanalysis to provide higher spatial resolution over Europe, employing the HARMONIE-ALADIN limited-area numerical weather prediction and data assimilation system.

Bittig et al. (2023) developed a measurement-based and model-assisted regional pCO_2 climatology, which is publicly available. For the present study, a more detailed dataset was provided, including monthly values for 2019 to 2021. The pCO_2 calculations used observations from the Surface Ocean CO_2 Atlas (SOCAT) database, which compiles measurements from voluntary observing ships, such as the Integrated Carbon Observation System Ships of Opportunity (ICOS SOOP), and re-

https://doi.org/10.5194/egusphere-2026-5442
Preprint. Discussion started: 10 September 2026

search vessels. The majority of the pCO_2 data were collected aboard the M/S Finnmaid, which operates between Travemünde, Germany and Helsinki, Finland. Bittig et al. (2023, 2024) performed modelling using empirical orthogonal functions (EOF) and the Ecological ReGional Ocean Model (ERGOM). Monthly pCO_2 maps were reconstructed by combining model output with observations.

The pCO_2 dataset included standard deviations, which were used to estimate the uncertainties of the calculated fluxes. In addition, a 20% uncertainty was incorporated into the gas transfer velocity parameterization, following the recommendation of Wanninkhof (2014). The uncertainty range was determined by recalculating the fluxes using pCO_2^{sea} values adjusted by one standard deviation and by applying a $\pm 20\%$ uncertainty to the gas transfer velocity parameterization.

Two gaps in the $p\mathrm{CO}_2$ dataset were filled to calculate annual fluxes. The January 2019 values differed considerably from the typical January $p\mathrm{CO}_2$ values, likely because of the small number of measurements. As interpolation from adjacent months was not possible at the beginning of the study period, the January 2019 values were replaced with the mean of January 2020 and 2021. The December 2020 data were completely missing and were replaced with the mean of November 2020 and January 2021.

2.3 STEAM

The Ship Traffic Emission Assessment Model (STEAM) utilizes Automatic Identification System (AIS) position reports to characterize global shipping activity. It integrates vessel movement data with technical specifications of the global fleet to predict performance, fuel consumption, air emissions, discharges, and underwater noise emissions, while accounting for ambient factors such as wind, waves, sea currents, and sea ice cover (Jalkanen et al., 2009, 2012; Johansson et al., 2013, 2017; Majamäki et al., 2025). STEAM applies water resistance calculations for performance prediction and supports detailed vessel-level modeling, which informs annual reporting of environmental pressures from shipping in the Baltic Sea region. In this study, STEAM v4.3.5 was employed to estimate CO_2 emissions using AIS data obtained from the Baltic Marine Protection Committee (HELCOM) data archive.

2.4 CIF-FLEXPART

The CIF-FLEXPART model (Mengistu et al., 2026), which is based on the Lagrangian atmospheric transport model FLEXPART v10.4 (Pisso et al., 2019) (Fig 3), was employed in this study. FLEXPART was operated in backward mode to generate hourly source–receptor relationships on a 0.2° latitude by 0.2° longitude grid over Europe (11°W to 34°E and 34°N to 72°N) and on a 2° by 2° global grid, using 10-day trajectories for each observation. Background conditions were estimated by coupling trajectory endpoints to three-dimensional mole fraction fields, which were obtained from the CAMS global inversion-optimized greenhouse gas fluxes and concentrations product, v22r2 for 2018–2022 and v23r1 for 2023. FLEXPART was driven by hourly ECMWF ERA5 reanalysis data at a 1° by 1° resolution and 137 vertical levels (Hittmeir et al., 2018).

CO_2 prior surface fluxes are optimised using the Community Inversion Framework (CIF), an open-source system designed to interface with multiple optimization schemes and atmospheric transport models (Berchet et al., 2021). The CIF four-dimensional variational (4DVAR) optimisation scheme is applied to minimise the Bayesian cost function.

https://doi.org/10.5194/egusphere-2026-5442
Preprint. Discussion started: 10 September 2026

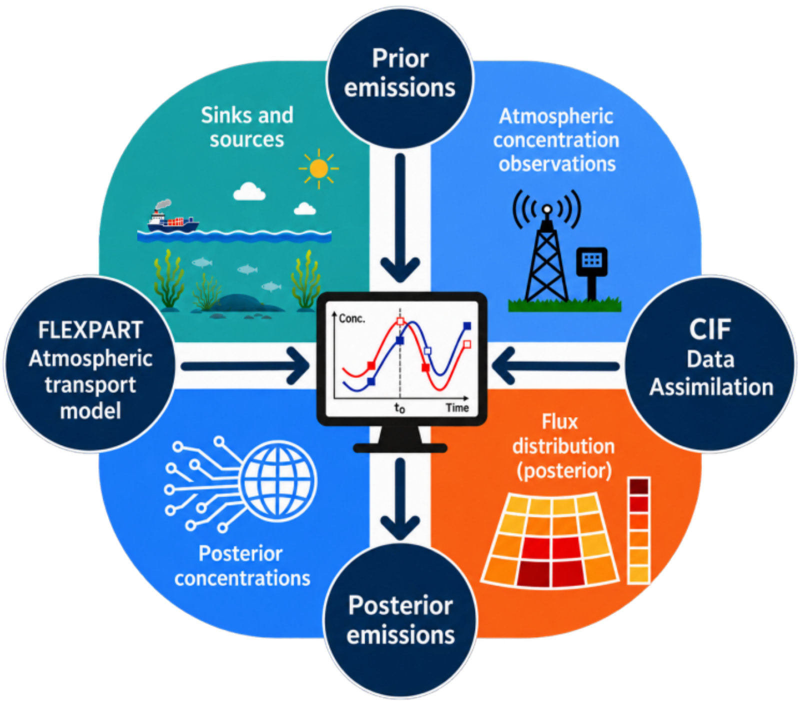

Figure 3. Schematic illustration of the CIF-FLEXPART inversion framework. Prior surface CO_2 fluxes are combined with atmospheric CO_2 observations through the FLEXPART atmospheric transport model and the CIF data assimilation system to optimize the prior fluxes and produce posterior surface CO_2 fluxes.

$$J(x) = \frac{1}{2}(x - x_b)^{\mathrm{T}} B^{-1}(x - x_b) + \frac{1}{2}(y_o - H(x))^{\mathrm{T}} R^{-1}(y_o - H(x)), \tag{4}$$

Here, x denotes the control vector of surface fluxes, x_b is the prior estimate with the associated error covariance matrix B, y_o represents the observed CO_2 mole fractions, and R denotes the observation error covariance matrix.

Efficient minimisation of the cost function requires computation of its gradient with respect to the control vector. This gradient is obtained using the adjoint of the transport operator H^{T} derived from FLEXPART:

$$\nabla J(x) = B^{-1}(x - x_b) - H^{\mathrm{T}} R^{-1}(y_o - H(x)), \tag{5}$$

which propagates mismatches between observed and modelled mole fractions back into the flux space.

https://doi.org/10.5194/egusphere-2026-5442
Preprint. Discussion started: 10 September 2026

CO_2 fluxes are categorized into four sectors, with three sectors optimized separately yet concurrently. The sectors and their associated uncertainties are as follows: oceans (100% uncertainty), anthropogenic (80%), and land net ecosystem exchange (NEE) (100%). Biomass burning fluxes are prescribed and not subject to optimization. Ocean fluxes are optimized daily, anthropogenic fluxes monthly, and land NEE every three hours for the period 2019 to 2021.

Global ocean prior fluxes are sourced from Jena CarboScope (s10oc_v2024E), provided at a spatial resolution of 2° × 2° and a daily temporal resolution. For the European domain, ocean fluxes are obtained from CarbonTracker Europe High-Resolution (CTE-HR, van der Woude et al. (2023)), which utilizes climatological Jena CarboScope fluxes to generate hourly fluxes at 0.1° latitude × 0.2° longitude resolution, based on wind speed and temperature fields. Anthropogenic prior fluxes are derived from EDGAR_2024_GHG (0.1° × 0.1°, monthly). These anthropogenic fluxes include emissions from shipping which are in the Baltic Sea in EDGAR_2024_GHG based on the STEAM model. Within the European domain, land net ecosystem exchange is obtained from the JSBACH–HIMMELI land ecosystem process-based model (0.125° × 0.125°, 3-hourly), driven by CRU-ERA5 climate data. Outside the European domain, land net ecosystem exchange fluxes are taken from the optimized biospheric land fluxes from CAMS global inversion-optimized greenhouse gas fluxes and concentrations v23r1. Biomass burning fluxes are sourced from GFAS v1.2 (0.1° × 0.1°, daily). All prior flux datasets are regridded to 0.2° × 0.2° over Europe and to 2° × 2° elsewhere.

Atmospheric CO_2 mole fraction measurements are taken from the European Obspack compilation, which includes CO_2 data from both ICOS and non-ICOS European ground-based continuous monitoring stations for the period 1972–2025 (obspack_co2_466_GVeu_v11_20250815, ICOS RI et al. (2025)). In total, measurements from 47 sites were incorporated into the inversion. ICOS observations are provided as hourly averaged mole fractions at 1-hour resolution. The inversion assimilates these hourly averages sampled every 3 hours (00, 03, 06, ..., 21), thereby utilizing information from the full diurnal cycle while maintaining a manageable observation volume. Unlike approaches that restrict assimilation to afternoon or nighttime observations, this strategy ensures more continuous temporal coverage and imposes additional constraints on surface fluxes. When measurements are available at multiple inlet heights at a given station, only data from the highest inlet are assimilated.

3 Results

For spatial analysis, the Baltic Sea was divided into sub-basins (Figure 1). The study area comprises the Danish Straits, Arkona Basin, Bornholm Basin, Gdansk Basin, Eastern Gotland Basin, Western Gotland Basin, Gulf of Riga, Northern Baltic Proper, Gulf of Finland, Åland Sea, Bothnian Sea, the Quark, and Bothnian Bay. The basin division follows the HELCOM subbasins as developed by Pemberton (2022).

The bulk air-sea CO_2 flux was calculated as illustrated in Fig. 2, yielding monthly flux values for 2019 to 2021. These values were adjusted using Copernicus sea ice data and the STEAM model, after which time series and mean net values were derived. The resulting dataset allows investigation of spatial and temporal variability in air-sea CO_2 flux.

Figure 4 presents the STEAM-corrected bulk method net CO_2 flux values for 2019 to 2021, both for the entire Baltic Sea and for each basin individually, along with associated uncertainties. The three-year mean CO_2 flux in the Baltic Sea during

https://doi.org/10.5194/egusphere-2026-5442
Preprint. Discussion started: 10 September 2026

this period is -1.79 $\mathrm{mmol\,m^{-2}\,d^{-1}}$ (uncertainty range: -21.9 to 11.8 $\mathrm{mmol\,m^{-2}\,d^{-1}}$), with annual means of -1.37, 1.57, and -5.58 $\mathrm{mmol\,m^{-2}\,d^{-1}}$. The annual mean fluxes among the 13 basins vary widely, ranging from -26.9 to 27.1 $\mathrm{mmol\,m^{-2}\,d^{-1}}$. Including ship emissions increased the Baltic Sea mean flux from -3.76 to -1.79 $\mathrm{mmol\,m^{-2}\,d^{-1}}$, representing a change of 1.97 $\mathrm{mmol\,m^{-2}\,d^{-1}}$.

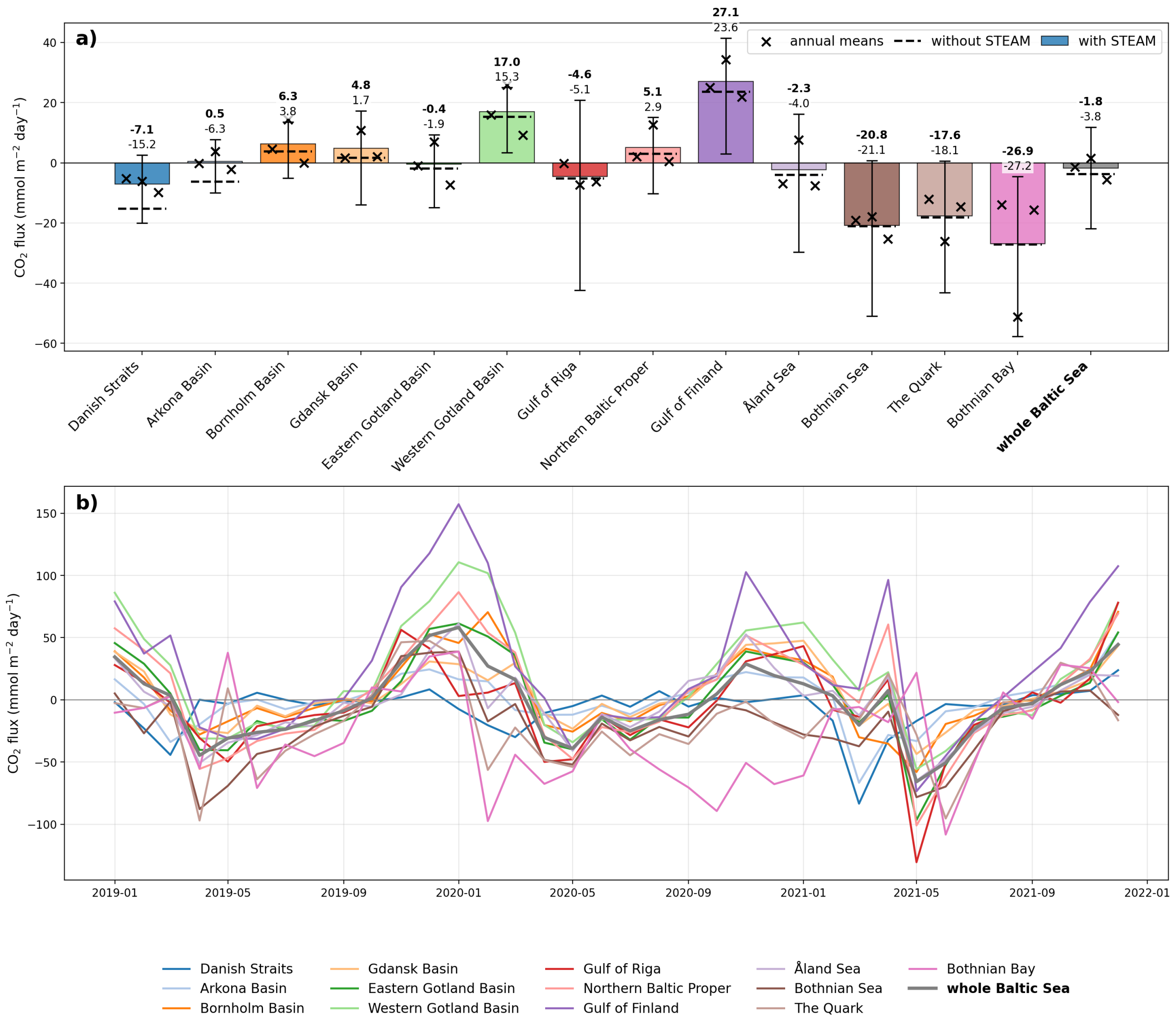

Figure 4. Bulk CO_2 flux estimates with and without STEAM ship emissions for each Baltic Sea basin during 2019–2021: (a) three-year mean net CO_2 fluxes including ship emissions (bars) and mean air–sea CO_2 fluxes excluding ship emissions (dashed lines). The crosses correspond to each year during the time period. Error bars indicate the estimated uncertainties, and the values above the bars denote the corresponding mean fluxes with (bold) and without the STEAM model. (b) Monthly mean net CO_2 flux time series for each basin.

Figure 4a demonstrates that the Gulf of Finland and the Western Gotland Basin represent the most significant sources of carbon dioxide, whereas the northern regions of the Baltic Sea act as strong carbon sinks. The impact of ship traffic emissions is

https://doi.org/10.5194/egusphere-2026-5442
Preprint. Discussion started: 10 September 2026

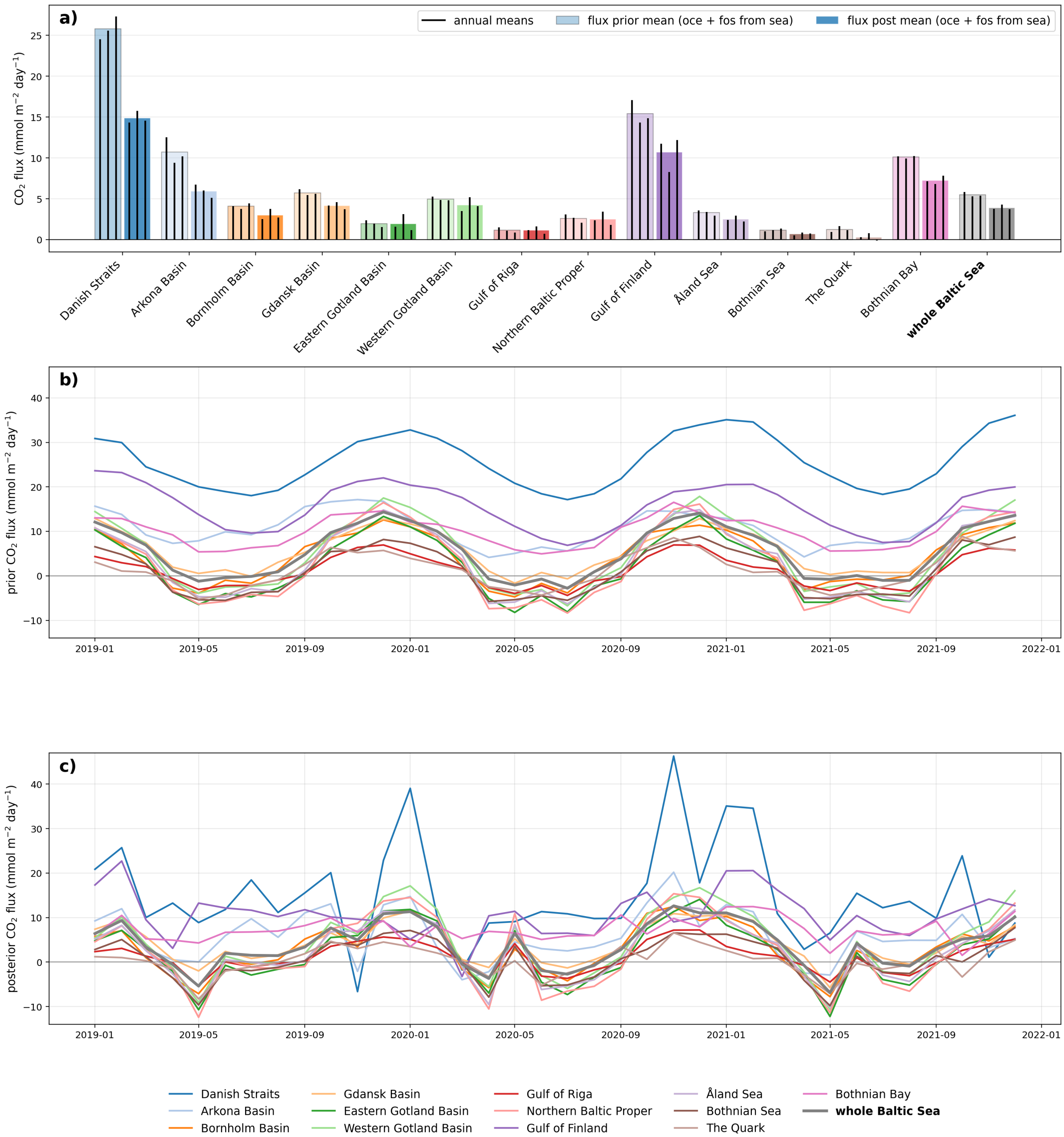

Figure 5. Inversion fluxes. The a) panel shows the mean prior and posterior fluxes by basin, using bars corresponding to those in the a) panel of Figure 4. The black lines overlaid on the wide bars indicate the annual mean values. Prior fluxes are shown in lighter colors, while posterior fluxes are shown in darker colors. The two lower panels present the time series of the prior (b) and posterior (c) fluxes for each basin. All data in this figure include oceanic and anthropogenic components of the inverse model.

https://doi.org/10.5194/egusphere-2026-5442
Preprint. Discussion started: 10 September 2026

most pronounced in the Danish Straits and the Arkona Basin, where the differences between mean bulk flux values calculated with and without the STEAM model are 8.13 and 5.83 $\mathrm{mmol\,m^{-2}\,d^{-1}}$, respectively. The STEAM contributions in Figure 4a are presented per unit area ($\mathrm{mmol\,m^{-2}\,d^{-1}}$), supporting direct comparison among basins of varying sizes.

Monthly bulk CO_2 fluxes, including ship emissions (Figure 4b), display generally consistent patterns across the basins. However, the Danish Straits, the Gulf of Finland, and the Bothnian Bay show clear deviations. The Danish Straits reach a minimum in March each year, differing from most other basins, and otherwise remain close to zero. The Gulf of Finland occasionally shows anomalously high fluxes compared with the other basins and the expected seasonal cycle, whereas the Bothnian Bay shows anomalously low values, particularly during autumn and winter 2021. Overall, the fluxes follow a clear seasonal cycle, with negative values (sink) in spring and summer and positive values (source) in autumn and winter. During summer, the fluxes are relatively similar between the basins, while the differences are larger in winter.

For comparison, corresponding climatological values were calculated using the bulk method and open-access data from Bittig et al. (2023), covering the period 2003 to 2021, as shown in Fig. A3. Since the STEAM model does not extend over this period, these estimates exclude ship emissions. The 18-year mean flux is 0.25 $\mathrm{mmol\,m^{-2}\,d^{-1}}$ (uncertainty range: -6.44 to 4.72 $\mathrm{mmol\,m^{-2}\,d^{-1}}$). Among the 13 basins, climatological mean fluxes range from -9.10 to 3.48 $\mathrm{mmol\,m^{-2}\,d^{-1}}$, which is narrower than the range observed for 2019 to 2021. This narrower range is also reflected in the time series (Fig. A3b), which presents the climatological monthly mean values.

Figure 5 presents results from the CIF-FLEXPART model. The three-year mean prior CO_2 flux for the study area is 5.50 $\mathrm{mmol\,m^{-2}\,d^{-1}}$, while the mean posterior flux is 3.92 $\mathrm{mmol\,m^{-2}\,d^{-1}}$. Both values account for oceanic and anthropogenic components. In contrast to the STEAM-corrected bulk method, positive annual fluxes are observed in all basins. The Eastern Gotland Basin is the only basin where the mean posterior flux slightly exceeds the mean prior flux, with a negligible difference of 0.001 $\mathrm{mmol\,m^{-2}\,d^{-1}}$. The most substantial change in mean flux is observed in the Danish Straits, where the posterior flux decreases by 10.9 $\mathrm{mmol\,m^{-2}\,d^{-1}}$.

The inverse model consists of two components: an oceanic component (Fig. A1) and an anthropogenic component (Fig. A2). The oceanic component demonstrates a pronounced seasonal cycle, particularly in the prior fluxes. The anthropogenic component is primarily positive in the prior estimates, although some basins also display seasonal variability. The anthropogenic posterior fluxes include seven months with negative values, which may suggest that the inversion has difficulty distinguishing shipping emissions from oceanic emissions. In both prior and posterior estimates, basin-mean oceanic fluxes remain close to zero, while the anthropogenic component shifts the total mean fluxes (oceanic plus anthropogenic; Fig. 5) substantially toward positive values.

The posterior flux time series (Fig. 5c) demonstrates a pronounced seasonal cycle in most basins. However, the Danish Straits, Gulf of Finland, and Bothnian Bay are notable exceptions. The Danish Straits have the highest monthly fluxes among the basins, with negative fluxes occurring in only two months during the three-year period. In the Gulf of Finland, the flux is negative during only one month, while no negative values occur in the Bothnian Bay. The temporal variation in the Arkona Basin also differs from that in most other basins. Analysis of the component-wise time series (Figs. A1 and A2) suggests that

https://doi.org/10.5194/egusphere-2026-5442
Preprint. Discussion started: 10 September 2026

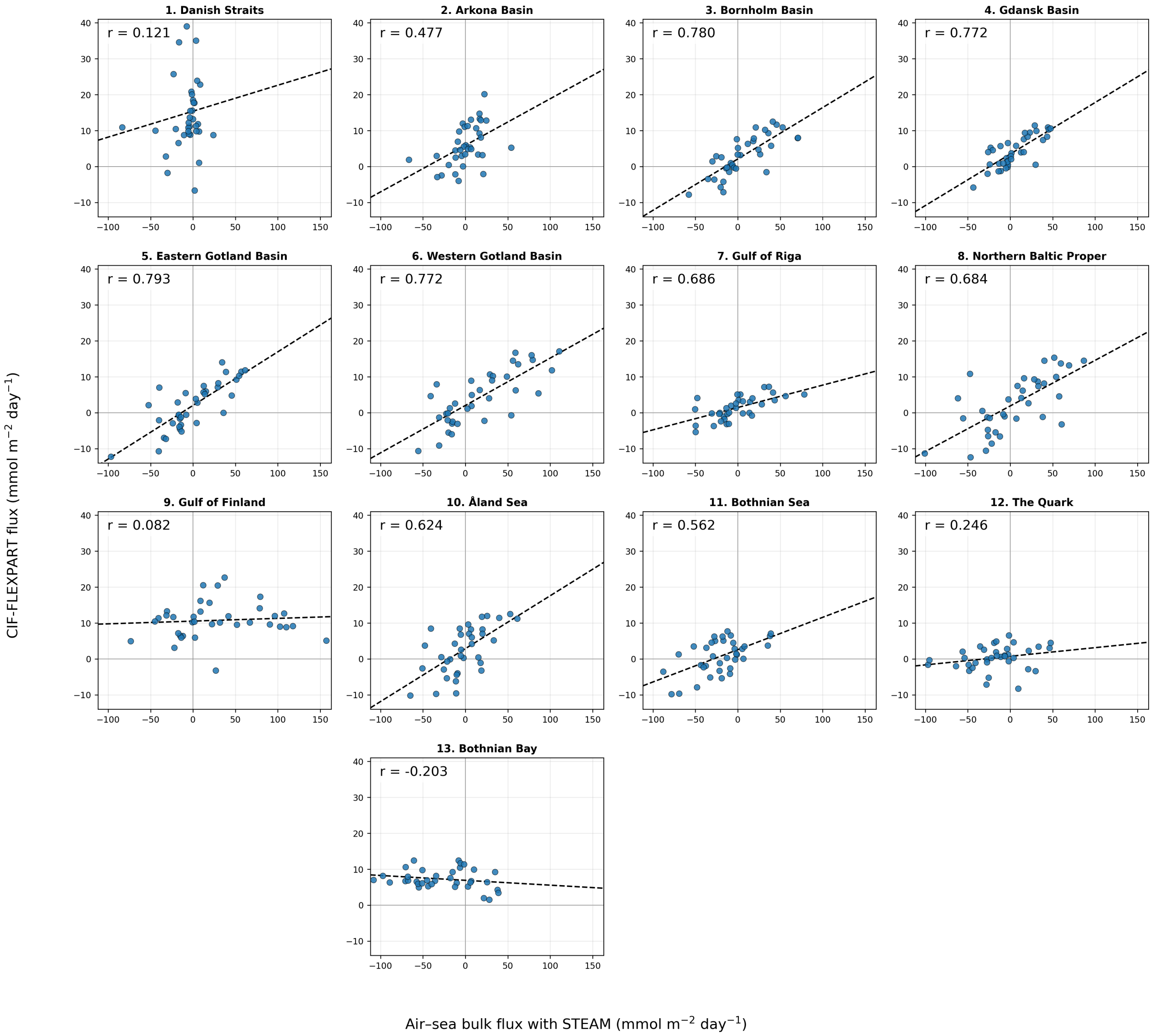

Figure 6. Basin-wise monthly net flux Pearson correlation between the STEAM-corrected bulk method and the inversion method posterior flux. The Pearson correlation coefficient is shown in the upper-left corner of each panel.

the anomalous behavior in these four basins is primarily attributable to the anthropogenic component. In contrast, the remaining nine basins exhibit broadly similar temporal variability and seasonal patterns.

The monthly variability of the inversion fluxes is lower than that of the STEAM-corrected bulk fluxes, with ranges from -12.4 to 46.3 (excluding the Danish Straits, up to 22.7) $\mathrm{mmol\,m^{-2}\,d^{-1}}$ and from -131 to 159 $\mathrm{mmol\,m^{-2}\,d^{-1}}$, respectively (Figs. 4–5). Despite this difference in variability, the three-year basin-wise mean fluxes presented in the bar graphs are of comparable magnitude to each other. Overall, the inverse model results show substantially more positive fluxes, suggesting a stronger CO_2 source than the fluxes derived using the STEAM-corrected bulk method. The largest difference in annual mean fluxes between

https://doi.org/10.5194/egusphere-2026-5442
Preprint. Discussion started: 10 September 2026

the calculation methods is observed in the Bothnian Bay, reaching 34.2 $\mathrm{mmol\,m^{-2}\,d^{-1}}$. Conversely, the smallest difference is found in the Gdansk Basin, at 0.67 $\mathrm{mmol\,m^{-2}\,d^{-1}}$.

In both time series (Fig. 5 b and c), peaks can be observed during midsummer (May or June), which correspond to the interval between the two summer phytoplankton blooms. This pattern is also evident in Fig. A1. In the prior flux estimates, this feature is relatively weak, but it becomes more pronounced following the inversion. In the STEAM-corrected bulk method time series (Fig. 4b), the timing of the spring bloom peaks varies between basins. In contrast, the posterior inversion time series (Fig. 5c) indicates that bloom peaks occur predominantly in the same month across all basins.

Figure 6 presents the Pearson correlations between basin-wise monthly net fluxes derived from the two methods. Substantial differences between the methods are evident across the basins. The strongest correlation is observed in the Eastern Gotland Basin ($r = 0.79$), while the weakest occurs in the Gulf of Finland ($r = 0.08$). In the Bothnian Bay, the correlation coefficient is negative ($r = -0.20$), indicating a weak inverse relationship between the two methods. In the latter two, almost all monthly posterior fluxes are positive. The mean correlation across all basins is $r = 0.49$.

Figure A4 displays the Pearson correlations between STEAM-corrected bulk fluxes and the prior fluxes from the inversion model. In all basins except the Danish Straits, the correlation coefficients are higher for the prior fluxes. The most pronounced difference occurs in the Gulf of Finland, where the correlation is $r = 0.71$ for the prior and $r = 0.08$ for the posterior. The overall Pearson correlation across all basins is $r = 0.65$, suggesting slightly stronger agreement between the STEAM-corrected bulk method and the prior fluxes compared to the posterior fluxes.

4 Discussion

The three-year mean air-sea CO_2 bulk flux (excluding STEAM) of -3.76 $\mathrm{mmol\,m^{-2}\,d^{-1}}$ demonstrates that the Baltic Sea functioned as a net sink of CO_2 during 2019 to 2021. When the STEAM ship-emission model is included, the mean STEAM-corrected bulk flux remains negative at -1.79 $\mathrm{mmol\,m^{-2}\,d^{-1}}$. In contrast, the CIF-FLEXPART inversion model posterior, which includes both oceanic and anthropogenic components, indicates a strongly positive flux of 3.92 $\mathrm{mmol\,m^{-2}\,d^{-1}}$ for the same period. The net flux for the entire Baltic Sea, as estimated by the STEAM-corrected bulk method, is of the same order of magnitude as values reported in previous studies (Kuliński and Pempkowiak, 2011; Gustafsson et al., 2014; Norman et al., 2013; Parard et al., 2017; Lansø et al., 2015; Gutiérrez-Loza et al., 2021). In comparison, the estimate without STEAM correction suggests a slightly stronger CO_2 sink than previously documented. The climatological mean value for 2003 to 2021, calculated using the bulk method, also falls within the range of these studies, although it does not include STEAM contributions, which were also not included in the previous studies.

Several uncertainties affect the interpretation of these results. The $p\mathrm{CO_2}$ data have relatively high uncertainties in some regions, which also affect the calculated air–sea CO_2 fluxes. The January 2019 data were replaced by the mean values of January 2020 and 2021, while the December 2020 values were interpolated from the adjacent months. Additionally, the pCO_2 data contain some locally large-error estimates, with up to 6497 grids exceeding a 200 μatm standard deviation, representing 3.2% of all valid grids. When unreliable values are limited to certain regions, a basin-by-basin analysis allows anomalous

https://doi.org/10.5194/egusphere-2026-5442
Preprint. Discussion started: 10 September 2026

basins to be identified without substantially affecting the interpretation of the other regions. However, temporally varying uncertainties are more challenging to address. The mean values of individual basins are also influenced by the chosen basin divisions. As illustrated in Fig. 1, the basin boundaries do not align precisely with the coastlines.

Areas with a high frequency of measurements exhibit reduced uncertainty in air-sea CO_2 flux estimates Bittig et al. (2024). The majority of pCO_2 data used for calculating the bulk air-sea CO_2 flux were collected by M/S Finnmaid, which operates between Lübeck-Travemünde and Helsinki. The vessel crosses the southern Danish Straits, Arkona, Bornholm, Western and Eastern Gotland Basins, the Northern Baltic Proper, and the western Gulf of Finland (basin numbers 1, 2, 4, 5, 6, 8, and 9 in Figure 1). The absolute uncertainties of the STEAM-corrected bulk fluxes in these regions, with the exception of the Gulf of Finland, are notably lower than in other basins.

The parameterization of the gas transfer velocity, k, is another source of uncertainty. Dong et al. (2026) found a season-dependent bias in k when conventional wind speed–based parameterizations are used. Accounting for sea state and surfactants resulted in a stronger seasonal cycle of air–sea CO_2 fluxes than with wind speed–based parameterizations. Dobashi et al. (2026), in turn, found that wind speed–based parameterizations may overestimate k under fetch-limited and high-wind conditions in coastal regions. The STEAM-corrected bulk method already shows large seasonal flux amplitudes, and the results of Dong et al. (2026) suggest that these amplitudes could be even larger. On the other hand, the results of Dobashi et al. (2026) suggest that fluxes may be overestimated in some coastal regions. The $p\mathrm{CO_2}$ climatology may also represent coastal waters less accurately than the open Baltic Sea, potentially underestimating the generally higher and more variable coastal $p\mathrm{CO_2}$ values and the resulting air–sea CO_2 fluxes.

Uncertainties are particularly pronounced in the northern basins. Specifically, the sub-basins of the Gulf of Bothnia (11, 12, and 13) display strongly negative mean fluxes. During the winter of 2020–2021, fluxes remained negative throughout the season in these regions, a result that may not be realistic and is likely attributable to insufficient measurements. Sustained negative flux would imply continuous photosynthetic uptake to maintain low pCO_2 levels, which is not reasonable during winter. When the northern basins are excluded from the calculation, the estimated net flux for the Baltic Sea during 2019–2021 is 5.46 $\mathrm{mmol\,m^{-2}\,d^{-1}}$. By comparison, the 2003–2021 climatology indicates that the Gulf of Bothnia basins functioned as net CO_2 sources of 2.84, 0.43, and 3.48 $\mathrm{mmol\,m^{-2}\,d^{-1}}$ from south to north, respectively.

Additional anomalous periods are observed in Quark and Bothnian Bay during May 2019 and February–March 2020. The Pearson correlation between the flux estimates is weak for these basins ($r = 0.25$ and $r = -0.20$, respectively; Fig. 6), indicating substantial differences between the flux estimates derived from the two methods. In contrast, Löffler et al. (2012) reported mean fluxes of 0.4 and -2.0 $\mathrm{mmol\,m^{-2}\,d^{-1}}$ for the Bothnian Bay and the Bothnian Sea, respectively, based on observations from 1999–2010. Similarly, Lansø et al. (2015) estimated fluxes of 0.8 and 0.5 $\mathrm{mmol\,m^{-2}\,d^{-1}}$ for the same basins. The inversion-derived posterior flux in the Bothnian Sea (0.72 $\mathrm{mmol\,m^{-2}\,d^{-1}}$) is in good agreement with values reported in previous studies, whereas the agreement is weaker in the Bothnian Bay. This suggests that inversion-based flux estimates may be useful when in-situ pCO_2 data are not available.

Outside the northern parts, in the main basin areas (basin numbers 2, 3, 5, 6, and 8) the STEAM-corrected mean bulk fluxes are slightly higher than expected, even in the absence of ship emissions. Thomas and Schneider (1999) estimated that the Baltic

https://doi.org/10.5194/egusphere-2026-5442
Preprint. Discussion started: 10 September 2026

Proper functioned as a net sink, with an average flux of -2.47 ± 0.25 $\mathrm{mmol\,m^{-2}\,d^{-1}}$ during 1995–1996. Similarly, Norman et al. (2013) reported a flux of -1.7 to -1.8 $\mathrm{mmol\,m^{-2}\,d^{-1}}$ for the same area in a 50-year model simulation. Kuss et al. (2006) found the Arkona Basin to be a sink of -9.86 $\mathrm{mmol\,m^{-2}\,d^{-1}}$ during 2003–2004, while Wesslander et al. (2010) reported fluxes of 6.4 and 4.5 $\mathrm{mmol\,m^{-2}\,d^{-1}}$ in the Bornholm Basin and Eastern Gotland Sea, respectively, for the period 1994–2008.

The STEAM-corrected bulk fluxes display notable interannual variability, with 2020 being particularly distinct (Fig. 4). For example, the Eastern Gotland Basin functioned as a net sink of CO_2 in 2019 and 2021, but acted as a CO_2 source in 2020. This basin is generally considered a CO_2 sink (Schneider et al., 2014), a pattern also reflected in climatological bulk fluxes (Fig. A3a). The annual net STEAM-corrected bulk fluxes were -1.37 $\mathrm{mmol\,m^{-2}\,d^{-1}}$ in 2019, 1.57 $\mathrm{mmol\,m^{-2}\,d^{-1}}$ in 2020, and -5.58 $\mathrm{mmol\,m^{-2}\,d^{-1}}$ in 2021. The oceanic inverse posterior fluxes for 2020 also differ substantially from those of other years. The corresponding annual mean fluxes for the Baltic Sea were 0.09, 1.26, and -0.06 $\mathrm{mmol\,m^{-2}\,d^{-1}}$, respectively (Fig. A1).

The CIF-FLEXPART inverse model also shows anomalous behaviour in some regions. The Danish Straits, Arkona Basin, Gulf of Finland, and Bothnian Bay show only weak seasonal variability, with mostly positive fluxes throughout the study period, except for a few months. Analysis of the component-wise time series suggests that this anomaly originates from the anthropogenic component of the inverse model (Fig. A2), which dominates over the oceanic component in these basins. Consequently, the fluxes in these basins exhibit weak Pearson correlations with the STEAM-corrected bulk method (Fig. 6), particularly in the Danish Straits ($r = 0.12$), Gulf of Finland ($r = 0.08$), and Bothnian Bay ($r = -0.20$). In contrast, the remaining basin time series display broadly similar temporal variability throughout the study period.

The prior fluxes display variability of a similar order of magnitude to the posterior fluxes, as excepted. The oceanic prior fluxes, derived from the CTE-HR, appear to represent the seasonal variability of the Baltic Sea CO_2 flux in a relatively conservative manner. The anthropogenic component of the inverse model dominates the total flux signal (Figs. A2 and A1), which partially obscures the natural seasonal variability in the posterior flux time series.

The Pearson correlation coefficients are relatively high in the southern basins, except for the Danish Straits, showing that the temporal variability is similar between the two methods in these regions. In both methods, the flux time series follow the expected seasonal cycle without the anomalous behavior seen in some other basins. Most $p\mathrm{CO_2}$ measurements are also concentrated in these regions, except for the Gdansk Basin, which likely contributes to the lower uncertainties of the STEAM-corrected bulk flux estimates. The relatively high correlations therefore indicate good agreement between the methods in regions with better observational coverage and where the inversion-derived fluxes follow the seasonal cycle well.

A notable feature of the results is the difference in the amplitudes of monthly and annual flux variability, as shown in Figs. 4 and 5, and also visible in Fig. 6. Most inversion posterior monthly fluxes range from approximately -5 to 15 $\mathrm{mmol\,m^{-2}\,d^{-1}}$, whereas the STEAM-corrected bulk method fluxes vary within about ±50 $\mathrm{mmol\,m^{-2}\,d^{-1}}$. The climatological monthly flux time series (Fig. A3) falls between these two, with a range from -15 to 20 $\mathrm{mmol\,m^{-2}\,d^{-1}}$ (without STEAM). Therefore, the amplitude of the posterior flux time series is nearly an order of magnitude smaller than that of the STEAM-corrected bulk method estimates. This is not totally unexpected, as the inversion framework has a coarser spatial resolution (0.2° × 0.2°) than the STEAM-corrected bulk method (0.1° × 0.1°). The oceanic prior used in the inversion is based on the CTE-HR product (0.1° × 0.2°), which is derived from the Jena CarboScope ocean CO_2 fluxes (2° × 2°), so the information content

https://doi.org/10.5194/egusphere-2026-5442
Preprint. Discussion started: 10 September 2026

of the prior is ultimately limited by the coarser-resolution source data. Additionally, the predefined uncertainties of inverse model components (oceans 100%, anthropogenic 80%, and net ecosystem exchange 100%) are substantial. Consequently, the estimated fluxes from the inversion method are smoother and less sensitive to fine-scale variability than the observation-based calculations.

Previous studies indicate that seasonal flux variations fall between the amplitudes derived from the inverse model and those calculated using the STEAM-corrected bulk method. Shipboard measurements by Thomas and Schneider (1999) estimated an annual flux range of approximately $\pm 20\ \mathrm{mmol\,m^{-2}\,d^{-1}}$. Using an atmospheric transport model, Lansø et al. (2015) reported a variation of roughly -10 to 15 $\mathrm{mmol\,m^{-2}\,d^{-1}}$, which aligns with the inversion-model results. Additionally, Honkanen et al. (2024) measured air–sea CO_2 exchange at Utö Island in the southern Archipelago Sea, observing a monthly mean variation of approximately -20 to 35 $\mathrm{mmol\,m^{-2}\,d^{-1}}$. In comparison to these estimates, the variability of the STEAM-corrected bulk method fluxes is relatively large. However, the latter two studies are based on multi-year averages.

Land–air CO_2 fluxes can also influence inversion-derived air–sea CO_2 fluxes. This effect is especially significant in the Baltic Sea, where the extensive coastline facilitates close interaction between terrestrial and marine atmospheric signals. Since land–air CO_2 fluxes are generally much larger than air–sea CO_2 fluxes, the atmospheric signal from marine fluxes is relatively weak. As a result, inversion-derived air–sea CO_2 fluxes are sensitive to uncertainties in atmospheric boundary conditions and transport from nearby land areas. This may become more important at coarse spatial resolution, where the land–sea boundary is less accurately represented. For instance, in the Danish Straits, the fragmentation of land and sea means that a 0.2°× 0.2°grid cell covers a highly heterogeneous area. This heterogeneity may contribute to the elevated inversion-derived fluxes observed in the Danish Straits (Fig. 5).

The Results section reports that the three-year mean contribution of STEAM ship emissions is 1.97 $\mathrm{mmol\,m^{-2}\,d^{-1}}$. The posterior anthropogenic flux from the inversion model is 3.53 $\mathrm{mmol\,m^{-2}\,d^{-1}}$, which differs substantially from the STEAM estimate, despite the anthropogenic prior being based on the EDGAR inventory, where Baltic Sea shipping emissions are derived from the STEAM model. The estimate of 2.8 $\mathrm{mmol\,m^{-2}\,d^{-1}}$ reported by Jalkanen et al. (2009) for the Baltic Sea in 2007 falls between these values. The analysis by Jalkanen et al. (2009) also includes the Kattegat region, an area with active ship traffic.

The estimated net air–sea CO_2 flux for the Baltic Sea should be considered indicative. As previously discussed, multiple factors influence the resulting mean flux, and Fig. 4 indicates that the uncertainty of the basin-wide estimate is substantial, with an error bar width of approximately 34 $\mathrm{mmol\,m^{-2}\,d^{-1}}$. The inverse model results are also indicative and should be interpreted with caution. The differences between the STEAM-corrected bulk method and the inverse model show that further observations and methodological development are needed to better constrain the Baltic Sea carbon budget. The climatological bulk flux estimates for the main basins are likely the most reliable, but they do not include the ship emissions estimated by the STEAM model. Overall, the results show the value of combining different approaches to better describe the spatial and temporal variability of CO_2 fluxes and the carbon budget of coastal seas such as the Baltic Sea.

https://doi.org/10.5194/egusphere-2026-5442
Preprint. Discussion started: 10 September 2026

5 Conclusions

Combined air–sea and ship-related CO_2 fluxes in the Baltic Sea for 2019–2021 were estimated using two approaches: a STEAM-corrected bulk method and atmospheric inversion modelling. The STEAM-corrected bulk method integrates the bulk air-sea flux estimates with STEAM ship emissions, whereas the inversion method estimates surface CO_2 fluxes using atmospheric transport modelling and CO_2 observations.

Both methods produced CO_2 flux time series with clear seasonal variability and broadly similar temporal patterns, although the amplitudes differed by nearly one order of magnitude in some basins. However, the two methods gave contrasting estimates of the net Baltic Sea CO_2 balance. The STEAM-corrected bulk method indicated a net sink of atmospheric CO_2 (-1.79 $\mathrm{mmol\,m^{-2}\,d^{-1}}$), whereas the CIF-FLEXPART inverse model indicated a net source (3.92 $\mathrm{mmol\,m^{-2}\,d^{-1}}$) during 2019–2021. Including STEAM ship emissions increased the bulk flux estimate by 1.97 $\mathrm{mmol\,m^{-2}\,d^{-1}}$, showing that ship emissions have an important effect on the estimated Baltic Sea CO_2 balance. However, the flux remains negative. Without ship emissions, the climatological bulk flux for 2003 to 2021 was closer to neutral at 0.25 $\mathrm{mmol\,m^{-2}\,d^{-1}}$. These results show that the estimated Baltic Sea carbon balance depends on both the method used and the inclusion of anthropogenic emissions. Therefore, the reported net fluxes should be regarded as indicative rather than definitive estimates.

Despite the differences in magnitude, both methods show many of the same large-scale features of the Baltic Sea carbon cycle. The overall correlation between the basin-wise mean fluxes is moderate, but the agreement is relatively strong in the southern and central Baltic basins. Thus, despite the differences in flux magnitude, the two methods show similar spatial patterns and regional variability in some parts of the Baltic Sea.

The results vary considerably among basins, and natural regional variability must be distinguished from potential methodological uncertainties and deficiencies. Continuous measurements are required to improve flux estimates and further develop the parameterizations used in bulk flux calculations. In particular, the large uncertainties in some basins indicate where additional marine CO_2 observations would be most beneficial. Atmospheric inversion models also require further refinement to improve the representation of atmospheric CO_2 transport and boundary conditions, particularly in coastal regions where land and sea interact. Although inversion modelling cannot replace in-situ observations, it provides an important complementary approach, especially where marine pCO_2 observations are sparse. Higher spatiotemporal resolution would further improve its applicability to heterogeneous coastal seas.

Long-term observations are also needed to follow changes in coastal carbon dynamics, as increasing wintertime runoff due to climate change may increase the transport of humus-rich water from land to coastal regions. Increased browning has been observed particularly in the Bothnian Bay (Kahru et al., 2026), showing that terrestrial and marine carbon budgets are closely connected. The substantial contribution of shipping also shows that anthropogenic emissions should be considered when assessing the regional carbon balance of the Baltic Sea. Overall, better estimates of the Baltic Sea carbon budget require long-term marine observations, complementary modelling approaches, and consideration of both natural and anthropogenic carbon fluxes.

https://doi.org/10.5194/egusphere-2026-5442
Preprint. Discussion started: 10 September 2026

Data availability.

The CERRA data are available from the Climate Data Store (Schimanke et al., 2021), and the Baltic Sea Physics data from the Copernicus Marine Service (Danish Meteorological Institute (DMI), 2023). The regional Baltic Sea $p\mathrm{CO_2}$ climatology is available from the PANGAEA data repository (Bittig et al., 2023).

Appendix A: Additional figures from bulk method and inverse model results

Oceanic and anthropogenic components of the inverse model results are presented in Figs. A1 and A2, respectively.

Climatological basin-wise bulk method CO_2 mean fluxes and timeseries 2003–2021 are presented in Fig. A3.

Basin-wise Pearson correlations between STEAM corrected bulk method and inverse model prior fluxes are presented in Fig. A4.

Author contributions.

CRediT author statements: Conceptualization: VK, MH, LL, TA, MT, J-PJ; Formal analysis: VK; Investigation: VK, MH, LL, TA, MT, J-PJ; Methodology: LL; Data curation: GR, HB, J-PJ, TA, MT, AM; Supervision: LL, MH; Visualization: VK; Writing – original draft: VK; Writing – review and editing: VK, MH, MT, AM, J-PJ, TA, LL, GR, HB.

Artificial intelligence was used to assist with editing the text.

Competing interests.

The contact author has declared that none of the authors has any competing interests.

Acknowledgements. The Surface Ocean CO_2 Atlas (SOCAT) is an international effort, endorsed by the International Ocean Carbon Coordination Project (IOCCP), the Surface Ocean Lower Atmosphere Study (SOLAS) and the Integrated Marine Biosphere Research (IMBeR) program, to deliver a uniformly quality-controlled surface ocean CO_2 database. The many researchers and funding agencies responsible for the collection of data and quality control are thanked for their contributions to SOCAT.

This work utilized data from several Integrated Carbon Observation System (ICOS) stations and data releases; we thank the station PIs, operators, and the ICOS Carbon Portal for making these observations accessible. Most of the pCO2 data used originate from M/S Finnmaid (PIs Henry Bittig, Gregor Rehder and Michael Glockzin). Also, M/S Tavastland (Anna Willstrand-Wranne and Tobias Steinhoff) observations are especially acknowledged.

This study has been conducted using E.U. Copernicus Marine Service Information; https://data.marine.copernicus.eu/product/BALTICSEA_MULTIYEAR_PHY_003_011/description, https://cds.climate.copernicus.eu/datasets/reanalysis-cerra-single-levels?tab=overview

https://doi.org/10.5194/egusphere-2026-5442
Preprint. Discussion started: 10 September 2026

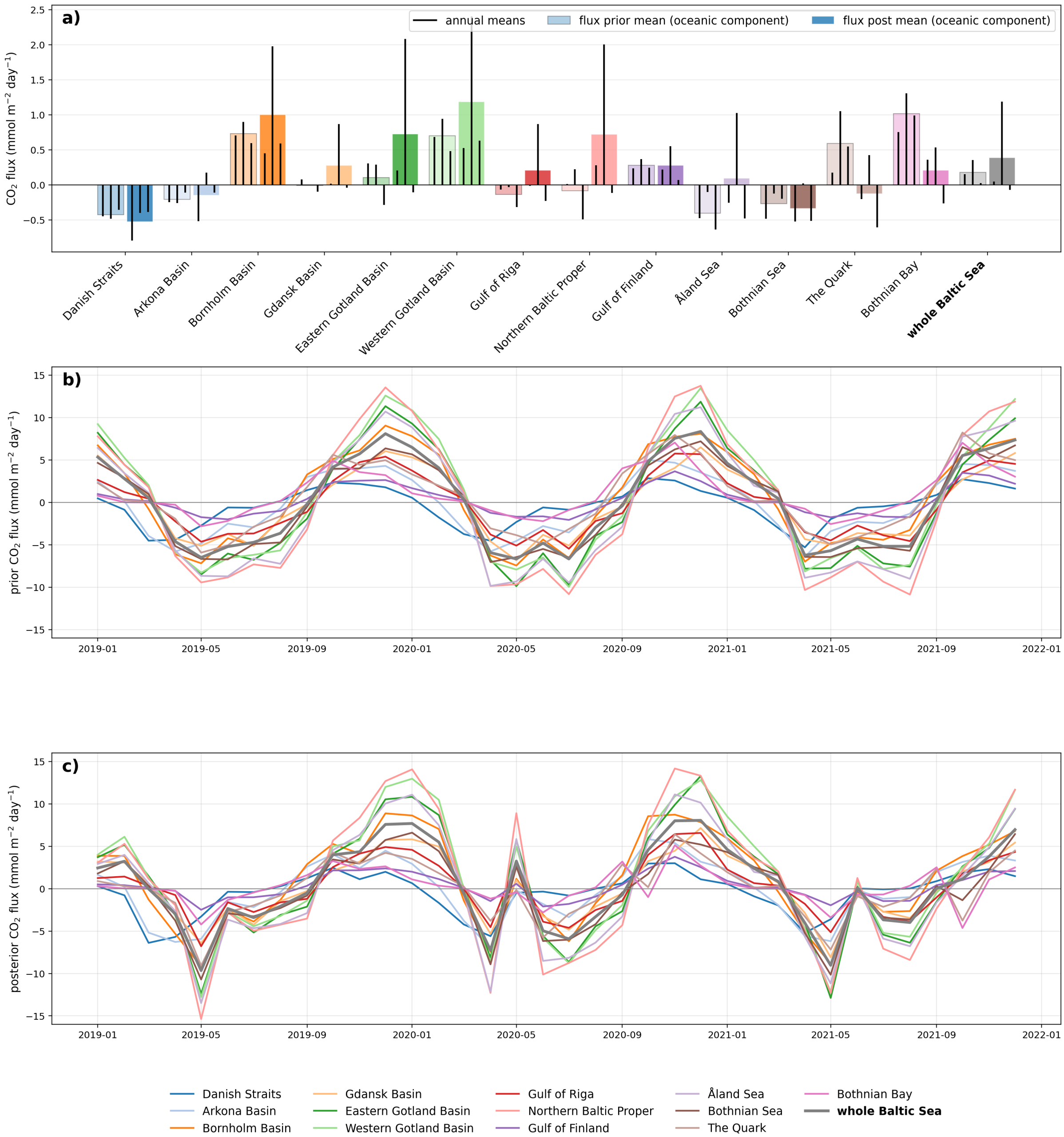

Figure A1. Corresponding to the Figure 5., but only oceanic component of inverse model. The a) panel shows the mean prior and posterior fluxes by basin, using bars corresponding to those in the a) panel of Figure 4. The black lines overlaid on the wide bars indicate the annual mean values. Prior fluxes are shown in lighter colors, while posterior fluxes are shown in darker colors. The two lower panels present the time series of the prior (b) and posterior (c) fluxes for each basin.

https://doi.org/10.5194/egusphere-2026-5442
Preprint. Discussion started: 10 September 2026

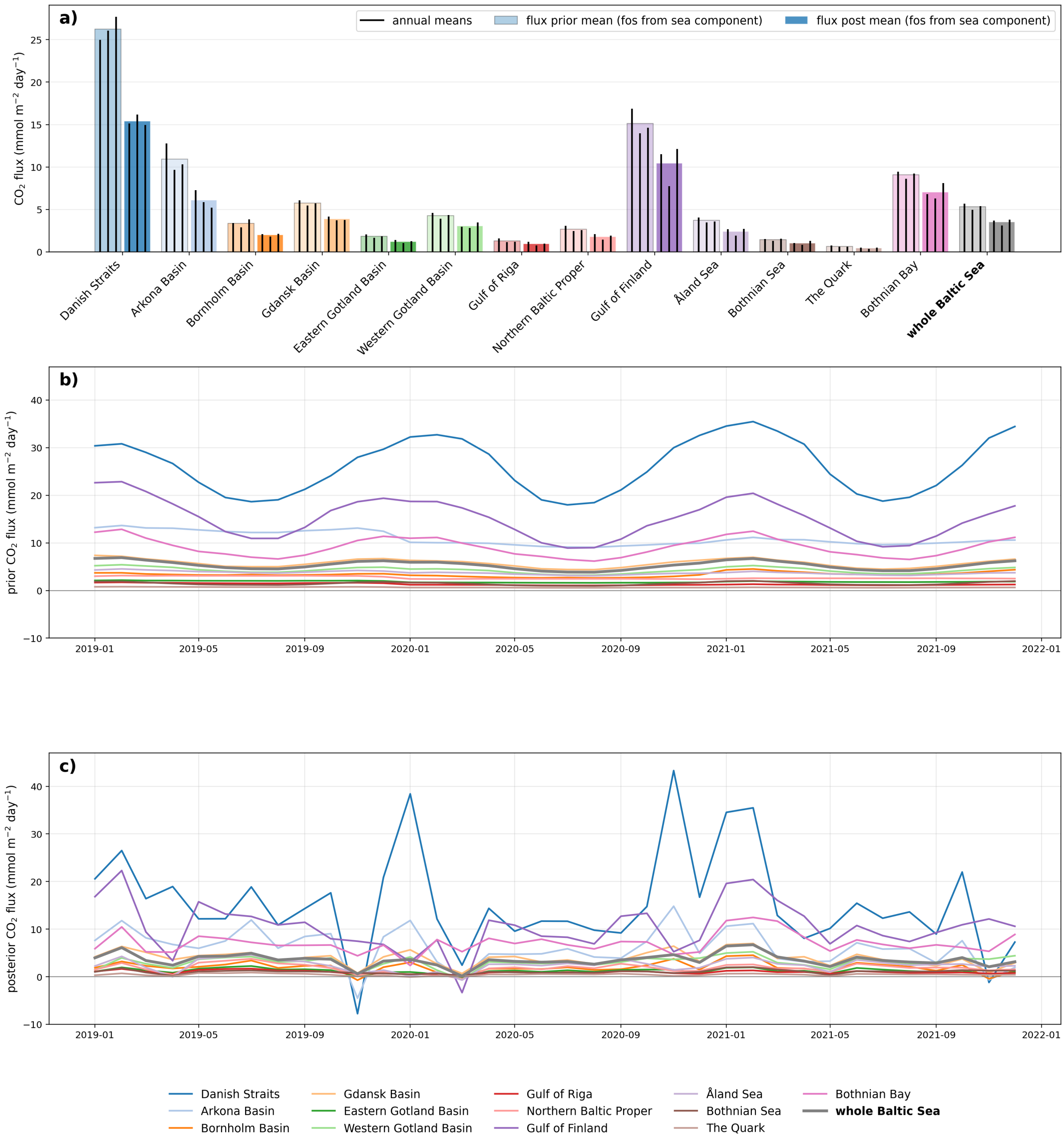

Figure A2. The same as Figure A1. above, but only the anthropogenic component of inverse model.

Baltic Sea pCO_2 climatology data from Bittig et al. (2024) were used in this study. The dataset is based on surface pCO_2 observations combined with ERGOM-derived variability patterns through a model-based extrapolation approach.

https://doi.org/10.5194/egusphere-2026-5442
Preprint. Discussion started: 10 September 2026

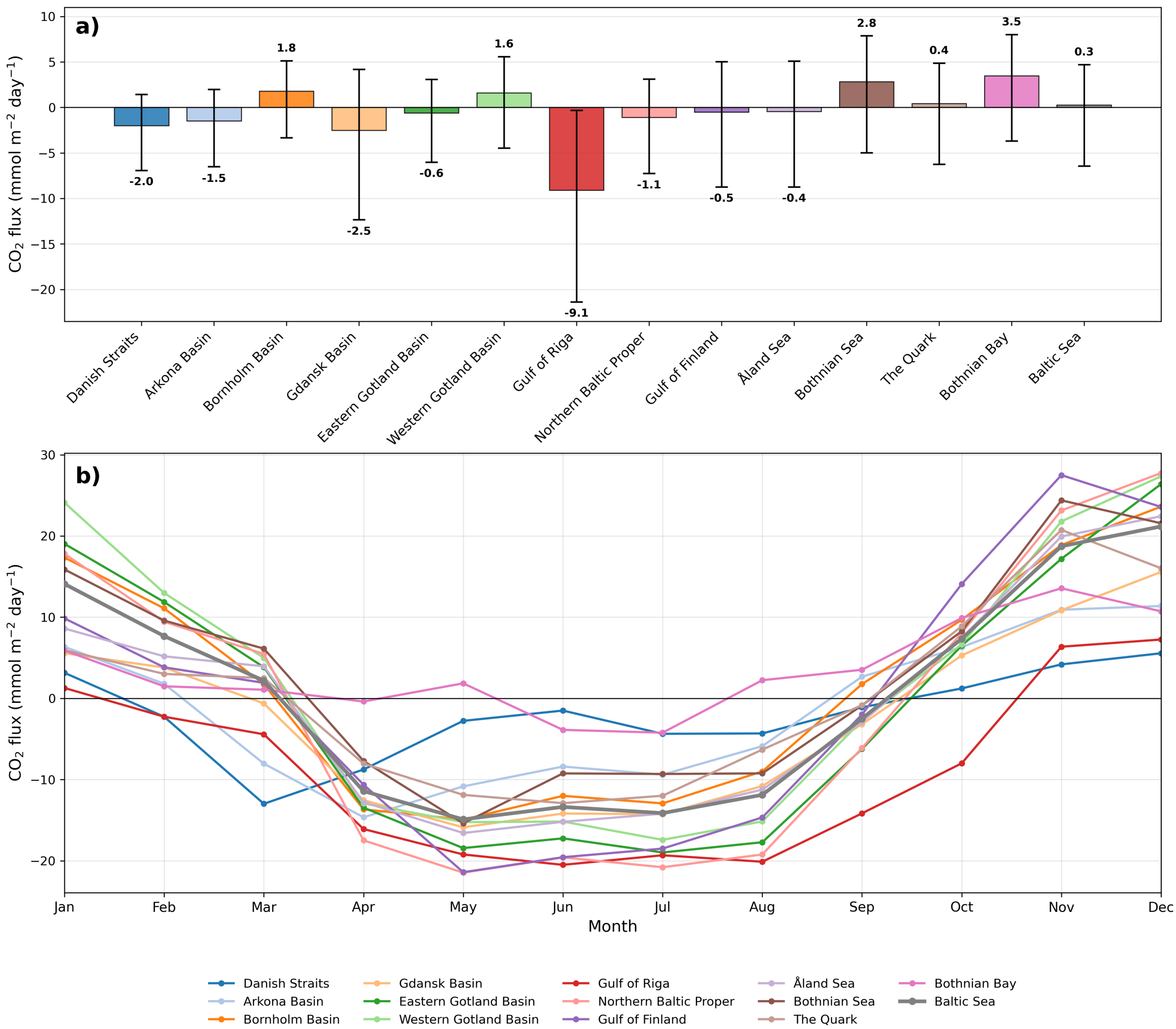

Figure A3. The same as Figure 4., but the climatological results from year 2003 to 2021. The STEAM model is not included in these results.

This work was supported by the the following projects: the Strategic Research Council at the Academy of Finland: Marine waterways as a sustainable source of well-being, security, and safety (Decision number: 365647); Verification System for the Green Transition (VISIO) project, the Just Transition Fund (JTF) under the EU regional and structural policy; Atmosphere and Climate Competence Center (ACCC) Flagship, the Research Council of Finland (grant nos. 359342 and 374289); the Finnish Marine Research Infrastructure (FINMARI, the Research Council of Finland, Research Infrastructure Roadmap 2025-2028 (grant no. 367725).

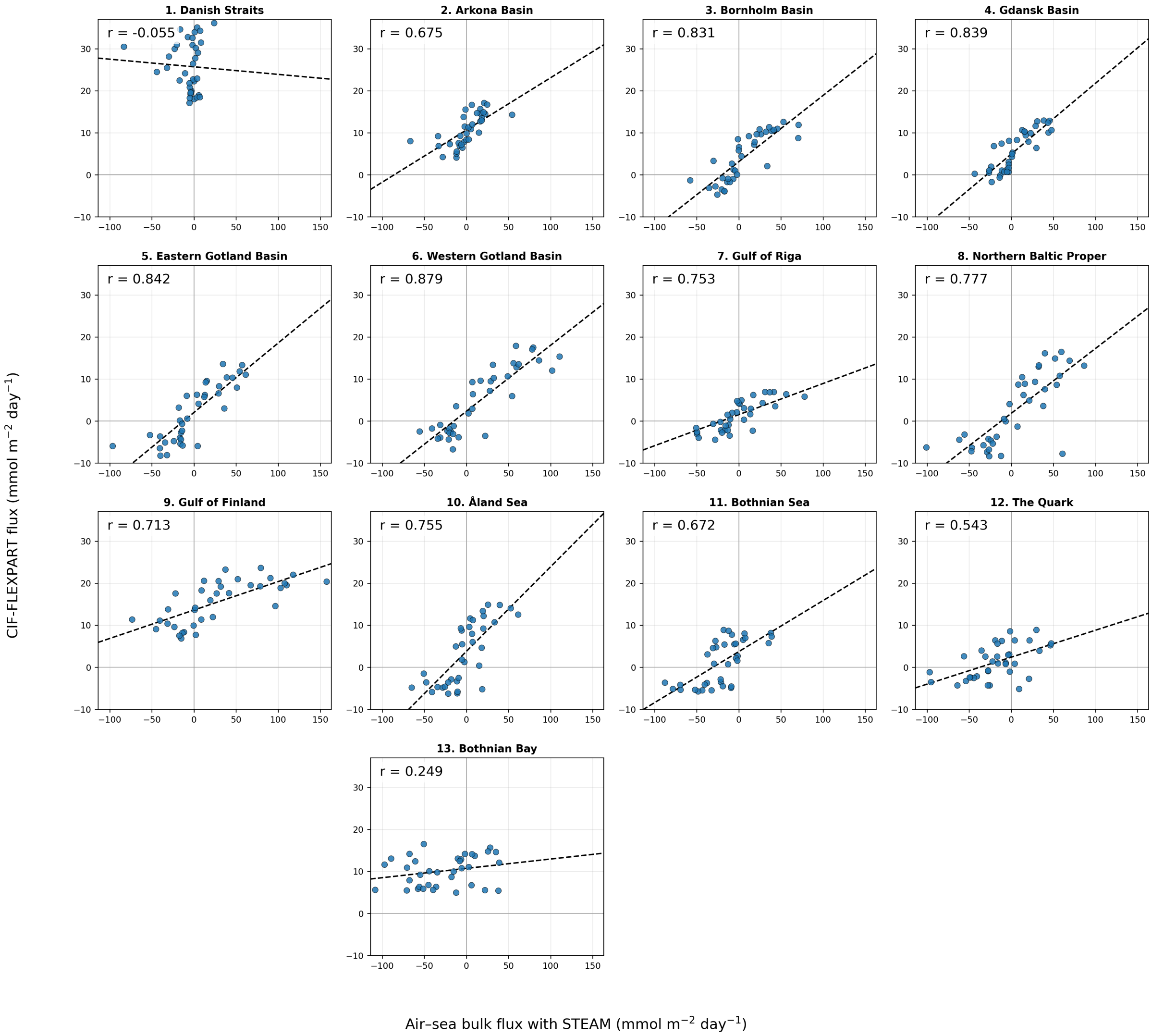

Figure A4. The same as Figure 6., but the inverse model prior fluxes.

References

455 Berchet, A., Sollum, E., Thompson, R. L., Pison, I., Thanwerdas, J., Broquet, G., Chevallier, F., Aalto, T., Berchet, A., Bergamaschi, P., Brunner, D., Engelen, R., Fortems-Cheiney, A., Gerbig, C., Groot Zwaaftink, C. D., Haussaire, J.-M., Henne, S., Houweling, S., Karstens, U., Kutsch, W. L., Luijkx, I. T., Monteil, G., Palmer, P. I., van Peet, J. C. A., Peters, W., Peylin, P., Potier, E., Rödenbeck, C., Saunois, M., Scholze, M., Tsuruta, A., and Zhao, Y.: The Community Inversion Framework v1.0: a unified system for atmospheric inversion studies, Geoscientific Model Development, 14, 5331–5354, https://doi.org/10.5194/gmd-14-5331-2021, 2021.

460 Bittig, H. C., Jacobs, E., Neumann, T., and Rehder, G.: A regional pCO_2 climatology of the Baltic Sea, https://doi.org/10.1594/PANGAEA.961119, 2023.

Bittig, H. C., Jacobs, E., Neumann, T., and Rehder, G.: A regional pCO_2 climatology of the Baltic Sea from in situ observations and model-based extrapolation, Earth System Science Data, 16, 753–773, https://doi.org/10.5194/essd-16-753-2024, 2024.

Bock, E. J., Hara, T., Frew, N. M., and McGillis, W. R.: Relationship between air–sea gas transfer and short wind waves, Journal of Geophysical Research, 104, 25 821–25 831, https://doi.org/10.1029/1999JC900200, 1999.

Chandra, N., Patra, P. K., Niwa, Y., Ito, A., Iida, Y., Goto, D., Morimoto, S., Kondo, M., Takigawa, M., Hajima, T., and Watanabe, M.: Estimated regional CO_2 flux and uncertainty based on an ensemble of atmospheric CO_2 inversions, Atmospheric Chemistry and Physics, 22, 9215–9243, https://doi.org/10.5194/acp-22-9215-2022, 2022.

Danish Meteorological Institute (DMI): E.U. Copernicus Marine Service Information (CMEMS); Baltic Sea Physics Reanalysis, https://doi.org/10.48670/moi-00010, accessed 28.7.2025, 2023.

Dickson, A. G., Sabine, C. L., and Christian, J. R.: Guide to Best Practices for Ocean CO_2 Measurements, PICES Special Publication 3, 2007.

Dobashi, R., Ho, D. T., Marandino, C. A., and Schlosser, P.: Air-Sea Gas Exchange in the Coastal Baltic Sea: Implications for Marine Carbon Dioxide Removal, Journal of Geophysical Research: Oceans, 131, e2025JC023 324, https://doi.org/10.1029/2025JC023324, 2026.

Dong, Y., Marandino, C. A., Dobashi, R., Ho, D. T., Rehder, G., Bittig, H. C., Karnatz, J., Sabbaghzadeh, B., Czerski, H., and Engel, A.: Mechanisms of Air–Sea CO_2 Exchange in the Central Baltic Sea, Atmospheric Chemistry and Physics, 26, 5567–5587, https://doi.org/10.5194/acp-26-5567-2026, 2026.

Friedlingstein, P., O'Sullivan, M., Jones, M. W., Andrew, R. M., Bakker, D. C. E., Hauck, J., Landschützer, P., Le Quéré, C., Li, H., Luijkx, I. T., Peters, G. P., Peters, W., Pongratz, J., Schwingshackl, C., Sitch, S., Canadell, J. G., Ciais, P., Aas, K., Alin, S. R., Anthoni, P., Barbero, L., Bates, N. R., Bellouin, N., Benoit-Cattin, A., Berghoff, C. F., Bernardello, R., Bopp, L., Brasika, I. B. M., Chamberlain, M. A., Chandra, N., Chevallier, F., Chini, L. P., Collier, N. O., Colligan, T. H., Cronin, M., Djeutchouang, L. M., Dou, X., Enright, M. P., Enyo, K., Erb, M., Evans, W., Feely, R. A., Feng, L., Ford, D. J., Foster, A., Fransner, F., Gasser, T., Gehlen, M., Gkritzalis, T., Goncalves De Souza, J., Grassi, G., Gregor, L., Gruber, N., Guenet, B., Gürses, O., Harrington, K., Harris, I., Heinke, J., Hurtt, G. C., Iida, Y., Ilyina, T., Ito, A., Jacobson, A. R., Jain, A. K., Jarníková, T., Jersild, A., Jiang, F., Jones, S. D., Kato, E., Keeling, R. F., Klein Goldewijk, K., Knauer, J., Kong, Y., Korsbakken, J. I., Koven, C., Kunimitsu, T., Lan, X., Liu, J., Liu, Z., Liu, Z., Lo Monaco, C., Ma, L., Marland, G., McGuire, P. C., McKinley, G. A., Melton, J. R., Monacci, N., Monier, E., Morgan, E. J., Munro, D. R., Müller, J. D., Nakaoka, S.-I., Nayagam, L. R., Niwa, Y., Nutzel, T., Olsen, A., Omar, A. M., Pan, N., Pandey, S., Pierrot, D., Qin, Z., Regnier, P., Rehder, G., Resplandy, L., Roobaert, A., Rosan, T. M., Rödenbeck, C., Schwinger, J., Skjelvan, I., Smallman, T. L., Spada, V., Sreeush, M. G., Sun, Q., Sutton, A. J., Sweeney, C., Swingedouw, D., Séférian, R., Takao, S., Tatebe, H., Tian, H., Tian, X., Tilbrook, B., Tsujino, H., Tubiello, F., van Ooijen, E., van der Werf, G. R., van de Velde, S. J., Walker, A. P., Wanninkhof, R., Yang, X., Yuan, W., Yue, X., and Zeng, J.: Global Carbon Budget 2025, Earth System Science Data, 18, 3211–3288, https://doi.org/10.5194/essd-18-3211-2026, 2026.

Gustafsson, E., Deutsch, B., Gustafsson, B. G., Humborg, C., and Mörth, C. M.: Carbon cycling in the Baltic Sea – The fate of allochthonous organic carbon and its impact on air–sea CO_2 exchange, Journal of Marine Systems, 129, 289–302, https://doi.org/10.1016/j.jmarsys.2013.07.005, 2014.

Gutiérrez-Loza, L., Wallin, M. B., Sahlée, E., Holding, T., Shutler, J. D., Rehder, G., and Rutgersson, A.: Air–sea CO_2 exchange in the Baltic Sea – A sensitivity analysis of the gas transfer velocity, Journal of Marine Systems, 222, 103 603, https://doi.org/10.1016/j.jmarsys.2021.103603, 2021.

https://doi.org/10.5194/egusphere-2026-5442
Preprint. Discussion started: 10 September 2026

Hittmeir, S., Philipp, A., and Seibert, P.: A conservative reconstruction scheme for the interpolation of extensive quantities in the Lagrangian particle dispersion model FLEXPART, Geoscientific Model Development, 11, 2503–2523, https://doi.org/10.5194/gmd-11-2503-2018, 2018.

Honkanen, M., Aurela, M., Hatakka, J., Haraguchi, L., Kielosto, S., Mäkelä, T., Seppälä, J., Siiriä, S.-M., Stenbäck, K., Tuovinen, J.-P., Ylöstalo, P., and Laakso, L.: Interannual and seasonal variability of the air–sea CO_2 exchange at Utö in the coastal region of the Baltic Sea, Biogeosciences, 21, 4341–4359, https://doi.org/10.5194/bg-21-4341-2024, 2024.

ICOS RI, Bergamaschi, P., Colomb, A., De Mazière, M., Emmenegger, L., Harris, E., Kubistin, D., Lehner, I., Lehtinen, K., Lund Myhre, C., Marek, M. V., Platt, S. M., Plaß-Dülmer, C., Rennick, C., Stanley, K., Zähle, S., Apadula, F., Arnold, S., Blanc, P.-E., Blessing, C., Brunner, D., Chen, H., Chmura, L., Conil, S., Couret, C., Cristofanelli, P., Forster, G., Frumau, A., Gerbig, C., Gheusi, F., Hammer, S., Haszpra, L., Hatakka, J., Heliasz, M., Henne, S., Hensen, A., Hoheisel, A., Jagoda, P., Joly, L., Kneuer, T., Larmanou, E., Laurila, T., Leskinen, A., Leuenberger, M., Levin, I., Lindauer, M., Lopez, M., Lunder, C., Mammarella, I., Manca, G., Manning, A., Martin, D., Meinhardt, F., Molnár, M., Mölder, M., Müller-Williams, J., Noe, S. M., Nęcki, J., O'Doherty, S., Ottosson-Löfvenius, M., Philippon, C., Pitt, J., Ramonet, M., Rivas-Soriano, P., Scheeren, B., Schumacher, M., Sha, M. K., Smith, P., Spain, G., Steinbacher, M., Sørensen, L. L., Vermeulen, A., Vítková, G., Xueref-Remy, I., Ylisirniö, A., di Sarra, A., Arriga, N., Conen, F., Kazan, V., Roulet, Y.-A., Biermann, T., Delmotte, M., Heltai, D., Hermansen, O., Komínková, K., Laurent, O., Levula, J., Marklund, P., Miettinen, P., Montaguti, S., Morguí, J.-A., Pichon, J.-M., Schmidt, M., Sferlazzo, D., Trisolino, P., Zazzeri, G., ICOS Carbon Portal, ICOS Atmosphere Thematic Centre, ICOS Flask And Calibration Laboratory, and ICOS Central Radiocarbon Laboratory: European Obspack compilation of atmospheric carbon dioxide data from ICOS and non-ICOS European stations for the period 1972-2025; obspack$_{c}o2_{4}66_{G}Veu_{v}11.0_{2}0250815$, https://doi.org/10.18160/$1NBR-4CM0$, 2025.

Jalkanen, J.-P., Brink, A., Kalli, J., Pettersson, H., Kukkonen, J., and Stipa, T.: A modelling system for the exhaust emissions of marine traffic and its application in the Baltic Sea area, Atmospheric Chemistry and Physics, 9, 9209–9223, https://doi.org/10.5194/acp-9-9209-2009, 2009.

Jalkanen, J. P., Johansson, L., Kukkonen, J., Brink, A., Kalli, J., and Stipa, T.: Extension of an assessment model of ship traffic exhaust emissions for particulate matter and carbon monoxide, Atmospheric Chemistry and Physics, 12, 2641–2659, https://doi.org/10.5194/acp-12-2641-2012, 2012.

Johansson, L., Jalkanen, J.-P. P., Kalli, J., and Kukkonen, J.: The evolution of shipping emissions and the costs of regulation changes in the northern EU area, Atmospheric Chemistry and Physics, 13, 11 375–11 389, https://doi.org/10.5194/acp-13-11375-2013, 2013.

Johansson, L., Jalkanen, J. P., and Kukkonen, J.: Global assessment of shipping emissions in 2015 on a high spatial and temporal resolution, Atmospheric Environment, 167, 403–415, https://doi.org/10.1016/j.atmosenv.2017.08.042, 2017.

Kahru, M., Cahill, B., Elovaara, S., Lee, Z., Rehder, G., Seppälä, J., Ylöstalo, P., and Zielinski, O.: Browning of the Baltic Sea, Marine Ecology Progress Series, 791, meps15 210, https://doi.org/10.3354/meps15210, 2026.

Kuliński, K. and Pempkowiak, J.: The carbon budget of the Baltic Sea, Biogeosciences, 8, 3219–3230, https://doi.org/10.5194/bg-8-3219-2011, 2011.

Kuss, J., Roeder, W., Wlost, K.-P., and DeGrandpre, M. D.: Time-series of surface water CO2 and oxygen measurements on a platform in the central Arkona Sea (Baltic Sea): Seasonality of uptake and release, Marine Chemistry, 101, 220–232, https://doi.org/https://doi.org/10.1016/j.marchem.2006.03.004, 2006.

https://doi.org/10.5194/egusphere-2026-5442
Preprint. Discussion started: 10 September 2026

Lansø, A. S., Bendtsen, J., Christensen, J. H., Sørensen, L. L., Chen, H., Meijer, H. A. J., and Geels, C.: Sensitivity of the air–sea CO_2 exchange in the Baltic Sea and Danish inner waters to atmospheric short-term variability, Biogeosciences, 12, 2753–2772, https://doi.org/10.5194/bg-12-2753-2015, 2015.

Leppäranta, M. and Myrberg, K.: Physical Oceanography of the Baltic Sea, Springer, 2009.

Löffler, A., Schneider, B., Perttilä, M., and Rehder, G.: Air–sea CO2 exchange in the Gulf of Bothnia, Baltic Sea, Continental Shelf Research, 37, 46–56, https://doi.org/https://doi.org/10.1016/j.csr.2012.02.002, 2012.

Majamäki, E., Johansson, L., Grönholm, T., and Jalkanen, J. P.: Improving the global prediction of shipping emissions by modelling the effects of ambient conditions, Science of the Total Environment, 997, 180 126, https://doi.org/10.1016/j.scitotenv.2025.180126, 2025.

Mengistu, A. G., Tsuruta, A., Berchet, A., Thompson, R., Tenkanen, M., Lindqvist, H., Markkanen, T., Leppänen, A., Laitinen, A., Martinez, A., Fortems-Cheiney, A., Höglund-Isaksson, L., and Aalto, T.: High-resolution inversion of methane emissions over Europe using the Community Inversion Framework and FLEXPART, EGUsphere, 2026, 1–41, https://doi.org/10.5194/egusphere-2025-5877, 2026.

Müller, J. D. and Schneider, B.: Biochemical Transformations in the Baltic Sea, Springer, 2018.

Norman, M., Rutgersson, A., and Sahlée, E.: Impact of improved air–sea gas transfer velocity on fluxes and water chemistry in a Baltic Sea model, Journal of Marine Systems, 111, 175–188, https://doi.org/10.1016/j.jmarsys.2012.10.013, 2013.

Parard, G., Rutgersson, A., Parampil, S. R., and Charantonis, A. A.: The potential of using remote sensing data to estimate air–sea CO_2 exchange in the Baltic Sea, Biogeosciences, 14, 5719–5737, https://doi.org/10.5194/bg-14-5719-2017, 2017.

Pemberton, P.: NEMO HELCOM masks, https://git.smhi.se/a001252/helcommasks, last modified: 24 May 2022, Last accessed 25 June 2026, 2022.

Pisso, I., Sollum, E., Grythe, H., Kristiansen, N. I., Cassiani, M., Eckhardt, S., Arnold, D., Morton, D., Thompson, R. L., Groot Zwaaftink, C. D., Evangeliou, N., Sodemann, H., Haimberger, L., Henne, S., Brunner, D., Burkhart, J. F., Fouilloux, A., Brioude, J., Philipp, A., Seibert, P., and Stohl, A.: The Lagrangian particle dispersion model FLEXPART version 10.4, Geoscientific Model Development, 12, 4955–4997, https://doi.org/10.5194/gmd-12-4955-2019, 2019.

Rutgersson, A., Norman, M., Schneider, B., Pettersson, H., and Sahlée, E.: The annual cycle of carbon dioxide and parameters influencing the air–sea carbon exchange in the Baltic Proper, Journal of Marine Systems, 74, 381–394, https://doi.org/10.1016/j.jmarsys.2008.02.005, 2008.

Rutgersson, A., Norman, M., and Åström, G.: Atmospheric CO_2 variation over the Baltic Sea and the impact on air–sea exchange, Boreal Environmental Research, 14, 238–249, https://doi.org/10.60910/c237-6jya, 2009.

Sarmiento, J. L. and Gruber, N.: Ocean Biogeochemical Dynamics, Princeton University Press, Princeton, NJ, ISBN 9780691017075, 2006.

Schimanke, S., Ridal, M., Le Moigne, P., Berggren, L., Undén, P., Randriamampianina, R., Andrea, U., Bazile, E., Bertelsen, A., Brousseau, P., Dahlgren, P., Edvinsson, L., El Said, A., Glinton, M., Hopsch, S., Isaksson, L., Mladek, R., Olsson, E., Verrelle, A., and Wang, Z. Q.: CERRA sub-daily regional reanalysis data for Europe on single levels from 1984 to present, Copernicus Climate Data Store, https://doi.org/10.24381/cds.622a565a, accessed 11.9.2025, 2021.

Schneider, B., Kaitala, S., and Maunula, P.: Identification and quantification of plankton bloom events in the Baltic Sea by continuous pCO2 and chlorophyll a measurements on a cargo ship, Journal of Marine Systems, 59, 238–248, https://doi.org/10.1016/j.jmarsys.2005.11.003, 2006.

Schneider, B., Gustafsson, E., and Sadkowiak, B.: Control of the mid-summer net community production and nitrogen fixation in the central Baltic Sea: An approach based on pCO2 measurements on a cargo ship, Journal of Marine Systems, 136, 1–9, https://doi.org/10.1016/j.jmarsys.2014.03.007, 2014.

https://doi.org/10.5194/egusphere-2026-5442
Preprint. Discussion started: 10 September 2026

Thomas, H. and Schneider, B.: The seasonal cycle of carbon dioxide in Baltic Sea surface waters, Journal of Marine Systems, 22, 53–67, https://doi.org/10.1016/S0924-7963(99)00030-5, 1999.

van der Woude, A. M., de Kok, R., Smith, N., Luijkx, I. T., Botía, S., Karstens, U., Kooijmans, L. M. J., Koren, G., Meijer, H. A. J., Steeneveld, G.-J., Storm, I., Super, I., Scheeren, H. A., Vermeulen, A., and Peters, W.: Near-real-time CO_2 fluxes from CarbonTracker Europe for high-resolution atmospheric modeling, Earth System Science Data, 15, 579–605, https://doi.org/10.5194/essd-15-579-2023, 2023.

Wanninkhof, R.: Relationship Between Wind Speed and Gas Exchange Over the Ocean, Journal of Geophysical Research, 97, 7373–7382, https://doi.org/10.1029/92JC00188, 1992.

Wanninkhof, R.: Relationship between wind speed and gas exchange over the ocean revisited, Limnology and Oceanography: Methods, 12, 351–362, https://doi.org/10.4319/lom.2014.12.351, 2014.

Wanninkhof, R. and McGillis, W. R.: A Cubic Relationship Between Air–Sea CO_2 Exchange and Wind Speed, Geophysical Research Letters, 26, 1889–1892, https://doi.org/10.1029/1999GL900363, 1999.

Weiss, A., Kuss, J., Peters, G., and Schneider, B.: Evaluating Transfer Velocity–Wind Speed Relationship Using a Long-Term Series of Direct Eddy Correlation CO_2 Flux Measurements, Journal of Marine Systems, 66, 130–139, https://doi.org/10.1016/j.jmarsys.2006.04.011, 2007.

Weiss, R. F.: The solubility of nitrogen, oxygen and argon in water and seawater, Deep-Sea Research, 17, 721–735, https://doi.org/10.1016/0011-7471(70)90037-9, 1970.

Weiss, R. F.: Carbon dioxide in water and seawater: The solubility of a non-ideal gas, Marine Chemistry, 2, 203–215, https://doi.org/10.1016/0304-4203(74)90015-2, 1974.

Wesslander, K., Omstedt, A., and Schneider, B.: Inter-annual and seasonal variations in the air–sea CO2 balance in the central Baltic Sea and the Kattegat, Continental Shelf Research, 30, 1511–1521, https://doi.org/10.1016/j.csr.2010.05.014, 2010.